Canadian **G**eothermal **S**tudents' **D**ay

Book of abstracts

Institut national de la recherche scientifique

Utica Resources

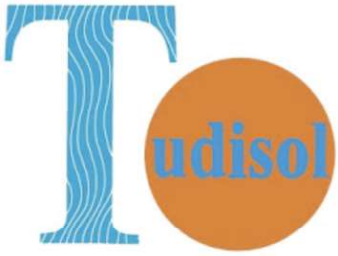

Centre d'études nordiques

Table of contents

Correlation between electrical resistivity and temperature and the impact of the seawater flow in the Asal rift, Republic of Djibouti.

Abdek Hassan Aden[1], Jasmin Raymond[1], Bernard Giroux[1]

[1] Institut national de la recherche scientifique, Québec, Canada

DOI: https://doi.org/10.5281/zenodo.3565925

Keywords: Correlation, hydrothermal, temperature and resistivity

Abstract

The main parameters influencing the variation of electrical resistivity in a rift context are temperature, the presence of fluids, the existence of hydrothermal alteration minerals and lithology. These parameters are mainly controlled by the volcanic and tectonic activity that determines the geological structure of the rift and the behavior of the associated hydrothermal system. Determining the predominant parameters that affect the electrical resistivity and its degree of influence over the other parameters is often tedious and sometimes subject to different interpretations, depending on the available data.

1. Introduction

The Magnetotelluric (MT) method has become a standard geophysical technique for subsurface exploration of geothermal fields. The evaluation of the Earth electrical conductivity allows to infer areas preferential to fluid flow. The objectives of this study are to advance the MT method by establishing a correlation between the variation of the temperature and electrical conductivity at depth, and to use the method to better understand how seawater flow influences the thermal behavior of hydrothermal systems in the Asal rift.

2. Methods and techniques

A series of 1D models of electrical resistivity will be developed from the inversion of MT data collected at 81 stations. A first correlation between the temperature profiles measured in geothermal wells and the variation in electrical resistivity of the stations closer to these boreholes will be performed. Then, a second correlation between the electrical resistivity and the estimated proportion of smectite in the drilling logs will be developed, since a high proportion of smectite is often interpreted as the cap rock of a geothermal reservoir.

Finally, a 2D multiphase flow model will be developed taking into account the regional groundwater flow with seawater that seeps through the open fractures of the Asal rift towards Asal Lake having an elevation difference of 153 m. Then, the influence of a magmatic heat source triggering the activation of hydrothermal systems overlying the regional flow will be evaluated.

3. Results and discussions

Our 1D model resistivity shows a good correlation between electrical resistivity and temperature profile measured in geothermal wells (**Fig. 1**). So, we infer the existence of two aquifers: the intermediate geothermal reservoir and the deep reservoir (**Fig. 1** and **Fig. 2**). The recharge and feeding of these aquifers come mainly from three types of sources: seawater, rainfall and water from Lake Asal. Generally, the water of hot springs of the Asal lake come from the varying degrees interaction of these three types of sources with the host rocks (basalts).

On the basis of the geochemical data, the initial fluid of hot springs located at North and South West of Lake Asal appears to be of meteoric origin. It is important to note also that some sources that are located North and South west of Asal Lake have an initial fluid that comes partially from Lake Asal (Sanjuan, 1990). A marine initial fluid feeds the hot springs in the axial part of the rift. This fluid, from the sea of Ghoubbet to Lake Asal, flows with high velocity into open fractures and fractures of the Asal rift (Mlynarski and al., 2001). The thermal anomaly beneath Asal rift increase the temperature of this fluid. Due the topography difference between the sea and the lake and properties of host rock, the hot springs are the evidence of this regional outflow.

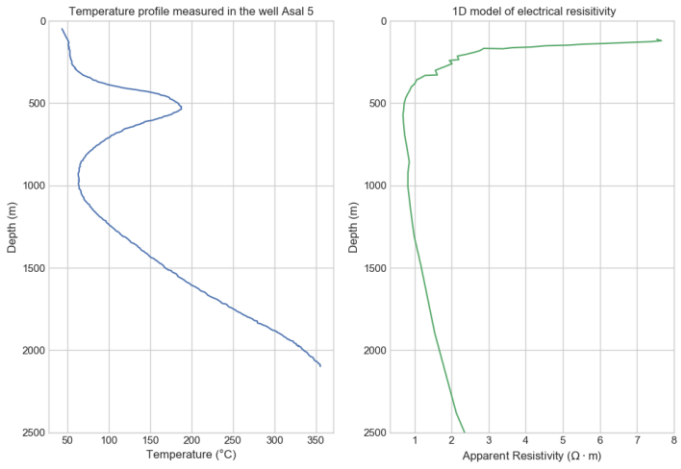

Fig. 1 Correlation between resistivity model and temperature profile measured in Asal 5.

Given the high salinity of Lake Asal and geochemical data, 90% of the water supply to Lake Asal is through this source of marine water.

The subsurface electrical conductivity of the region is mainly controlled by the groundwater flow and high heat flow under rift. We suggest that an intermediate reservoir exist and is associated with the low value around 1 ohm.m of electrical resistivity model between 500 and 1000 m of depth correspond the decrease of temperature profile that confirm the circulation of cold seawater. The increase of electrical resistivity under 1300 m and the correspond linearly geothermal gradient can be interpreted that the heat transfert is mainly dominated by conduction in the rocks and there is no any advection as confirm by drillings results of well Asal 5. The decrease of the electrical resistivity under 4000 m of depth (**Fig. 2**), may be due the presence of molten rock (Doubre et al., 2007) or a deep groundwater flow in permeable volcanic rocks.

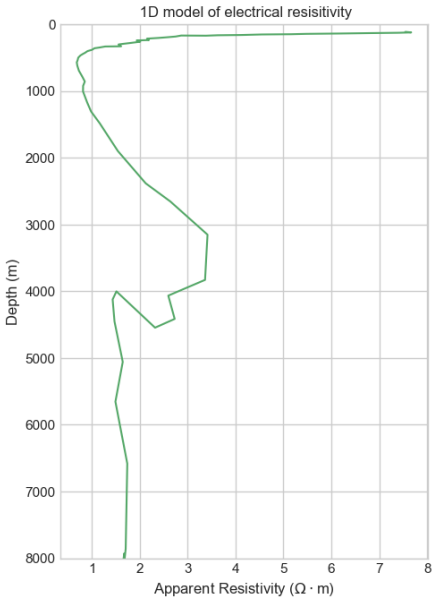

Fig. 2 Inversion model of the electrical resistivity of the closer MT station of Asal 5

4. Conclusions

Two geothermal reservoirs have been identified in the Asal rift by previous studies. Our results will clarify the role of the interpretation of the electrical resistivity in the characterization of the hydrothermal system and the understanding of the temporal evolution of the circulation of the sea water with the numerical modeling of multiphase flow and heat transfer.

Acknowledgements

We are aknowledged Dr. Bernard Sanjuan (BRGM), Gaten Sakindi (Electricity Company of Rwanda), Abdourahman Haga and Djama Robleh (Ministry of Energy and Natural Ressources of the Republic Djibouti) who contributed to this project. We also thank the IDB and the INRS for the scholarship of this project doctoral.

References

Doubre, C. and Peltzer, G.: Fluid-controlled faulting process in the Asal Rift, Djibouti, from 8 yr of radar interferometry observations, Geology, 35(1), 69–72, 2007.

Mlynarski, M. and Zlotnicki, J.: Fluid circulation in the active emerged Asal rift (east Africa, Djibouti) inferred from self-potential and Telluric–Telluric prospecting, Tectonophysics, 339(3–4), 455–472, 2001

Sanjuan, B., Michard, G. and Michard, A.: Origine des substances dissoutes dans les eaux des sources thermales et des forages de la région Asal-Ghoubbet (République de Djibouti), J. Volcanol. Geotherm. Res., 43(1–4), 333–352, 1990.

Tintina fault core analysis for potential geothermal development

Bennett Braun[1], Jonathan Banks[1]

[1.] University of Alberta, Department of Earth Sciences, Edmonton, Canada

DOI: https://doi.org/10.5281/zenodo.3565963

Abstract

A 500m exploratory well was drilled in the Ross River region in the Yukon to determine if the area warrants further geothermal research. The well is located along a laterally extensive dextral strike-slip fault, named the Tintina fault. Core analyses were conducted to evaluate the potential for development as a geothermal system. A geothermal gradient of 30.6°C/km was measured by a thermistor line. There is discussion of developing a greenhouse that can be heated by a direct use geothermal system, with the aim of reducing emissions from importing fresh produce, and to provide employment for the community.

1. Introduction

Canada currently generates no electricity from geothermal power, however there is some direct use for district heating applications (Raymond et al., 2015). Direct usage of geothermal energy in the Yukon is largely limited to simple systems to keep water from freezing, and for recreational hot springs. Yukon's energy is heavily based on hydroelectric power generation, and research being conducted is revealing large scale application and utilization of geothermal power. Many remote communities still exist as dependents on diesel as the only source of energy generation, and emissions could be mitigated by the substitution of geothermal power. Exploration along the Tintina fault through the Ross River test well has produced invaluable insight, and development of the area should be considered. The trench serves as a natural catchment for pre-glacial, glacial, and inter-glacial sediments spanning the late Pliocene to the late Pleistocene (Duk-Rodkin et al., 2010). These sediments are exposed and studied through land scars, but the regional geology is complex and generalized. The physical control on the sediments is limited, so geophysical information is utilized heavily. Acquiring data from core analyses of the Ross River test well gives insight into the hydrogeologic characteristics, and thermal properties at depth.

2. Methods and techniques

The well was drilled with a RC drill, to a depth of 500m. A thermistor line was lowered into the well with nodes at 10m intervals to measure temperature (Fraser, Colpron, & Relf, 2019). A variety of analyses were conducted: core logging, qualitative XRD, thin section analysis, and helium pycnometry.

3. Results

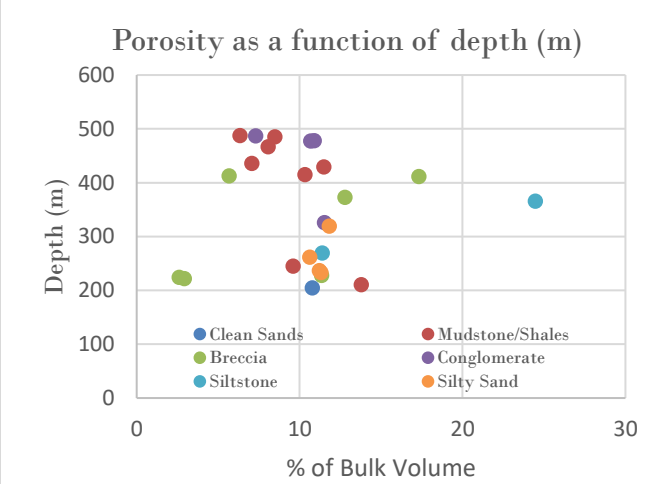

Fig. 1 Porosity of the Ross River well core samples as a function of depth, separated by lithology.

In the results, we observed relatively high porosity values in the samples. The values ranging from 2.6-25%. The XRD results expressed common minerals such as quartz, plagioclase, k-feldspar, muscovite, and chlorite in nearly all samples. However, clays such as kaolinite and smectite were not present in the breccia and silty sand units. On the other hand, all the other lithologies contained clays. Thin section analysis revealed many natural fractures, and prevalent vuggy porosity. A thermal gradient of 30.6°C/km was measured.

4. Discussion

The aim of this exploration project was to determine if the results warrant further geothermal research in the region. The geothermal gradient reflects it is indeed a region of elevated temperature, and could be developed as a resource. The Ross River people have expressed interest in developing a geothermal system to sustain the heat requirements of a greenhouse. A greenhouse would provide fresh produce to the community, and would reduce the emissions caused from importing food.

5. Conclusions

In conclusion, this study has proven the Ross River test well area to be a potential region for development as a geothermal resource. In collaboration with the Yukon Geological Survey, and the Ross River people, the project is moving forward.

Acknowledgments

Thank you to the University of Alberta, Government of Canada, Yukon Geological Survey, and the Ross River Dena Council for making this project possible.

References

Raymond, J., Malo, M., Tanguay, D., Grasby, S., & Bakhteyar, F. (2015). Direct Utilization of Geothermal Energy from Coast to Coast: a Review of Current Applications and Research in Canada. In *Proceedings World Geothermal Congress*.

Duk-Rodkin, A., Barendregt, R. W., & White, J. M. (2010). An extensive late Cenozoic terrestrial record of multiple glaciations preserved in the Tintina Trench of west-central Yukon: stratigraphy, paleomagnetism, paleosols, and pollenThis is a companion paper to Barendregt et al., also in this issue.Geological S. *Canadian Journal of Earth Sciences*, *47*(7), 1003–1028. https://doi.org/10.1139/e10-060

Fraser, T., Colpron, M., & Relf, C. (2019). Evaluating geothermal potential in Yukon through temperature gradient drilling. In *Yukon Geological Research Yukon Exploration and Geology*.

An approach to obtain g-functions using artificial neural networks

Bernard Dusseault[1]

[1.] Polytechnique Montreal, Civil, Geological and Mining Department, Montreal, Canada
bernard.dusseault@polymtl.ca

DOI: https://doi.org/10.5281/zenodo.3565969

Keywords: Neural Networks, g-Function, Geothermal Heat Exchangers, Vertical Closed Loop Systems

Abstract

G-functions are mathematical tools that link average borehole wall temperatures in borehole fields to heat injection and extraction rates. Various numerical, analytical and empirical ways to determine g-functions have been proposed by authors throughout the years. In this article, a way of assessing g-functions using artificial neural networks (ANN) is explored. This method is versatile enough to accommodate a varying number of boreholes and irregular borehole placements. The training of this ANN required half a million g-functions. Once trained, g-functions could be approximate in 0.19 second with an average precision of 0.285 % compared to reference g-functions.

1. Introduction

The objective is to measure the g-function approximation precision of ANN. Based on previous works (Dusseault and Pasquier 2018; Dusseault and Pasquier 2019), an architecture of three hidden layers with 200, 200 and 45 neurons respectively were chosen for the ANN (**Fig. 1**). It uses an input of 50 neurons to capture the geological and physical properties of the borehole field and uses 40 neurons to sample the resulting approximated g-function.

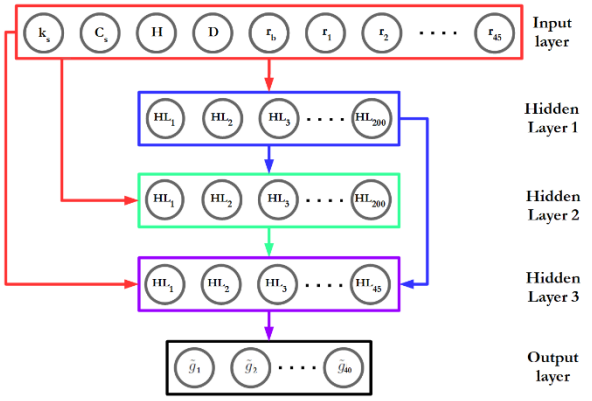

Fig. 1 Architecture of the ANN used in this work.

2. Methods and techniques

To validate the accuracy of the ANN's, 10 000 g-functions of 100 years were calculated. These approximations were compared against a benchmark of reference g-functions obtained through another established assessment method (Dusseault and al. 2017).

3. Results

The following **Table 1** shows the accuracies of the approximated g-functions for the best, median and worst of the validation cases. The average computation time of individual g-functions was 0.19 second.

Table 1 Accuracy of the approximated g-functions.

Relative accuracy	Value
Best case (%)	0.036
Median case (%)	0.285
Worst case (%)	2.450

4. Discussion

The configuration that led to the best case in **Table 1** consists of a single borehole while the one that led to the worst case consists of 9 boreholes distributed at random on a 20 m by 25 m grid. This demonstrates that while ANN are promising, there is still work to be done to broaden their approximation qualities for more complex GHEs.

5. Conclusions

G-functions placed irregularly within geothermal heat exchangers can be approximated quite rapidly, in 0.19 second on average, by ANN without sacrificing much accuracy, with errors ranging from 0.036% to 2.45%. This was proven by a comparative benchmark of 10 000 approximations by the ANN against an already published g-function assessment method.

References

Dusseault, B., P. Pasquier, and D. Marcotte. (2017). "A block matrix formulation for efficient g-function construction". Renewable Energy, Volume 121, pages 249–60.

Dusseault, B., and P. Pasquier. (2018). "Near-instant g-function construction with artificial neural networks". Proceedings of the IGSHPA Research Track 2018, Stockholm, Sweden, September 18–20.

Dusseault B., Pasquier P. (2019). "Efficient g-function approximation with artificial neural networks for a varying number of boreholes on a regular or irregular layout". Science and Technology for the Built Environment, Volume 25(8), pages 1023-1035.

A spatial-temporal study of the microbial-geochemical responses associated with groundwater heat pump systems

Charis Wong[1], Geneviève Bordeleau[1], Jasmin Raymond[1], Christine Rivard[2], Jérôme Comte[1]

[1]Institut national de la recherche scientifique, Centre – Eau Terre Environnent, Quebec, Canada
[2]Geological Survey, Natural Resources Canada – Quebec Division, Canada
Charis.wong@ete.inrs.ca

DOI: https://doi.org/10.5281/zenodo.3565973

Keywords: geothermal, open loop, aquifer, microbial, geochemical

Abstract

This project investigates the microbial and chemical responses to an eventual development and operation of groundwater heat pump systems, which make use of aquifer fluid for energy-efficient cooling of buildings in Quebec City. This involves understanding the change in microbial and chemical properties of the aquifer fluid as it travels through the system, along with the associated implications toward groundwater quality and equipment performance. Optimization of potential resource and equipment performance will also be investigated. Due to the early stage of this project, this short paper outlines the current overall concept and plan for the project.

1. Introduction

A substantial amount of heat is released into the atmosphere as a result of conventional building cooling methods. This contributes to the formation of urban heat island over time, which is expected to become a significant issue with climate change. Akbari (2005) shows that for every 1°C increase in air temperature above 22°C in Los Angeles, smog incidence is increased by 5%. This project investigates the potential of groundwater heat pump (GWHP) systems as a form of energy efficient cooling in Quebec City, with a specific focus on microbial and chemical responses resulting from the development and operation of such technology (Figure 1).

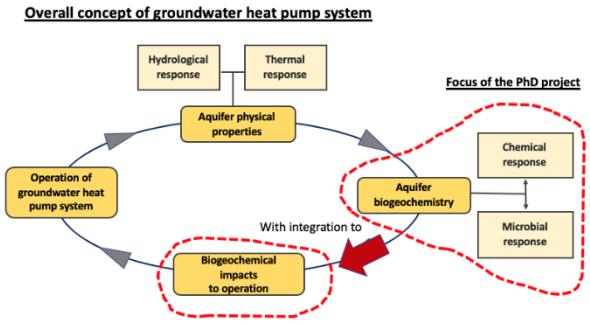

Fig. 1 Biogeochemical impacts to groundwater heat pump systems

With the operation of GWHP systems, aquifer fluid is extracted from groundwater wells and is used for cooling buildings, before being injected back into the aquifer. Because the fluid warms up as it cools the buildings, fluid temperature in the injection well is higher than in the extraction well. While open-loop systems are more efficient and more economical than closed-loop systems, potential concerns with this type of design include microbial-induced corrosion and clogging, mineral precipitation, and growth of pathogenic microorganisms, both in the system components themselves, and in the aquifer. These impacts may result from: 1) an increased temperature of the injected fluid, 2) mixing of fluids with different redox conditions during pumping, 3) changing redox conditions of the fluid as it flows through the system, 4) microbial dispersal due to injection, and 5) changes in the chemical-physical environment of microorganisms in the aquifer (Bonte et al. 2013, Griebler et al. 2016 and Burté et al. 2019). In order to assess the potential implications, it is important to understand how the different controlling factors influence the chemical and microbial properties of the fluid as it travels through the system.

2. Project concept and research objectives

This project is organized into three parts.
Part 1 aims to understand the chemical and microbial responses as aquifer fluid travels through different stages of an GWHP system (Figure 2), taking into consideration different factors such as seasonal variation (Zhou et al. 2012), aquifer formation type (Bai et al. 2016; Maamar et al. 2015), flow rate (Taylor et al. 2004), relation between bacterial cell properties and transport/retention (Bai et al. 2016, McBumett et al. 2018), and suspended versus attached bacteria in aquifer (Lehman et al. 2001). This will be achieved through various laboratory experiments.
Part 2 aims to integrate the knowledge of biogeochemical responses gained through the laboratory work and use it to predict impacts on groundwater quality (i.e. pathogenic bacteria *legionella*) and equipment performance (e.g.: microbially-induced corrosion/ clogging).
Part 3 aims to propose avenues for mitigating implications and optimising potential resource and

equipment performance. This will be done by applying knowledge obtained towards developing criteria for appropriate system design and optimal operational regime (such as optimal injection fluid temperature with consideration of mineral solubility or well casing depth to avoid mixing of shallow oxic and deeper anoxic fluids (Possemiers et al. 2016).

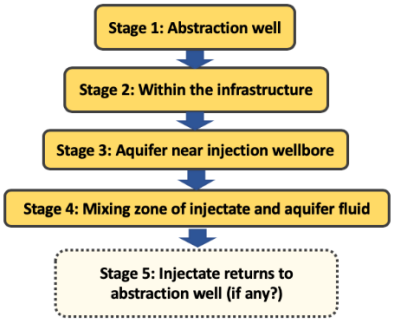

Fig. 2 Transportation of aquifer fluid through different stages of the GWHP system

3. Methods

In order to achieve the objectives mentioned above, this project will involve fieldwork (including aquifer characterisation and pilot tests), laboratory column experiments and reactive transport modelling (Figure 3).

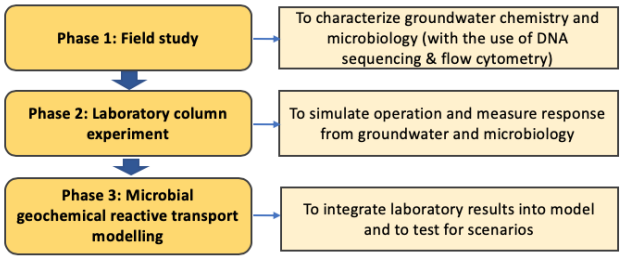

Fig. 3 Three main phases of the project

4. Conclusions

To mitigate the presence of urban heat islands which are amplified as a result of conventional cooling methods, the potential of groundwater heat pump system as a form of energy efficient cooling method will be investigated. This project will assess the microbial and chemical responses of such heat pump systems within the system components, and in the surrounding aquifer. This project aims to:

- Determine the controlling factors that influence the chemical and microbial properties of the aquifer fluid as it travels through the system.
- Understand the associated microbial and chemical impacts towards groundwater quality and equipment performance.
- Apply knowledge obtained towards mitigation of implications and optimization of resource and equipment.

5. Acknowledgments

This research is funded by the Natural Sciences and Engineering Research Council of Canada under the program Advancing Climate Change Science in Canada.

References

Akbari, H. (2005) "Potentials of urban heat island mitigation", Paper presented at the Conference "Passive and Low Energy Cooling for the Build Environment", May 2005, Santorini, Greece.

Bai H. et al. (2015) "Bacteria cell properties and grain size impact on bacteria transport and deposition in porous media", Colloids Surf., B, 139, 148-155.

Bonte M. et al. (2013) "Impacts of shallow geothermal energy production on redox processes and microbial communities", Environ. Sci. Technol., 47, 14476-14484.

Burté L et al. (2019) "Kinetic study on clogging of a geothermal pumping well triggered by mixing-induced biogeochemical reactions", Environ. Sci. Technol., 53, 5848-5857.

Griebler C. et al.. (2016) "Potential impacts of geothermal energy use and storage of heat on groundwater quality, biodiversity, and ecosystem processes", Environ. Earth Sci., 75, 1391.

Lehman R.M. et al. (2001) "Attached and unattached microbial communities in a simulated basalt aquifer under Fracture- and Porous-flow conditions", Appl. Environ. Microbiol., 67, 2799-2809.

Maamar S.B. et al. (2015) "Groundwater isolation governs chemistry and microbial community structure along hydrologic flowpaths", Front. in Microb., 6. 1457.

McBurnett L.R. et al. (2018), "Legionella – A threat to groundwater: pathogen transport in recharge basin", Sci. of Total Environ., 621, 1485-1490.

Possemiers M. et al. (2016) "Reactive transport modelling of redox processes to assess Fe(OH)3 precipitation around aquifer thermal energy storage wells in phreatic aquifers", Environ. Eart. Sci., 75, 648.

Taylor R. et al. (2004) "The implication of groundwater velocity variations on microbial transport and wellhead protection – review of field evidence", FEMS Microbiol. Ecol., 49, 17-26.

Zhou Y. et al. (2012) "Spatio-temporal patterns of microbial communities in hydrologically dynamic pristine aquifer", FEMS Microbiol. Ecol., 81, 230-242.

Aquifer characterization by active heat tracer using direct push fiber optics

Cynthia Lee[1], Nataline Simon[2], Jérôme de la Bernardie[2], Jean-Marc Ballard[1], Olivier Bour[2], René Lefebvre[1]

[1.] Institut national de la recherche scientifique, Centre Eau Terre Environnement, 490 rue de la Couronne, Québec, Canada
[2.] Univ Rennes, CNRS, Géosciences Rennes, UMR 6118, 35000 Rennes, France

DOI: https://doi.org/10.5281/zenodo.3565975

Keywords: active heat tracing, fiber optics DTS, aquifer characterization

Abstract

The potential and limitations of heat tracing using fiber optics active Distributed Temperature Sensing (DTS) were tested at three sites in the Valcartier deltaic aquifer under natural flow conditions. The sites were selected on the basis of different expected ranges of horizontal groundwater fluxes. Fiber optics cables collocated with Cone Penetration Tests (CPT) were installed by direct push adjacent to soil cores and observation wells. Heat tracing quantified groundwater fluxes and thermal properties, which were compared to lab and field measurements. Preliminary results indicate that the temperature profiles are correlated with the stratigraphy defined by the CPT soundings.

1. Introduction

Despite their potential, temperature and heat tracing have seldom been used to characterize aquifers and develop hydrogeological numerical models (Anderson, 2005). Recent advances in fiber optics and Distributed Temperature Sensing (DTS) systems have opened new possibilities for the use of temperature in hydrogeology, which has led to renewed interest in heat tracing (Selker et al., 2006; Bakker et al., 2015; Bense et al., 2016; des Tombe, 2019). However, the approaches to be used to get the full benefit from DTS still require further developments. The Valcartier deltaic aquifer is well suited for studying the potential of fiber optic DTS because it has been extensively studied due to a major trichloroethylene contamination problem (Ouellon et al., 2008 & 2010).

2. Methods and techniques

The Valcartier heat tracing experiment involved a wide range of complementary field and lab work aiming to assess both the potential and limitations of heat tracing using active DTS under natural flow conditions: direct push installation of fiber optics at three sites with different expected ranges of groundwater flux, cone penetration tests (CPT) collocated with fiber optics to provide high-resolution stratigraphic profiles, soil coring to measure thermal and hydraulic properties in the lab, direct push long-screened well to measure hydraulic properties, and downgradient observation wells to compare the velocity of groundwater to the indications provided by DTS.

At Site B, the repeatability of fiber optics DTS for the estimation of groundwater fluxes was tested. Two fiber optic cables, FO-B1 and FO-B2, were installed 10-meters apart by direct push. Active DTS was performed by heating the steel sheath around each fiber optic cable. The cable was heated for 73 hours, after which steady state was assumed to have been reached. The resulting thermal responses can be used to characterize both hydraulic flow and thermal properties along vertical profiles.

3. Results & Discussion

Preliminary results show that active heating can generate changes that are detectable with fiber optic DTS within the temperature profile. Figure 1 below shows the temperature response at four different depths along the fiber optic cable installed at site FO-B2. The hydraulic properties at each of these depths are different, as the material belongs to a different hydrofacies based on their CPT response.

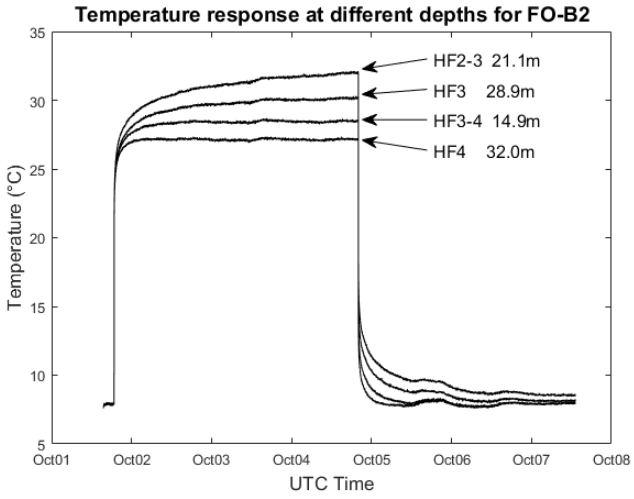

Fig. 1 Temperature response curves at depths with different aquifer materials as characterized by their CPT response corresponding to a distinct hydrofacies (HF); HF4 and HF2 have respectively the coarsest and finest grain sizes. Hydrofacies classification used the method developed by Fauveau (2006) (see also Ouellon et al., 2008).

Fig. 1 shows that the temperature response varies according to the different hydrofacies vertically present along the fiber optics DTS cable. More data interpretation is needed to explain this correlation, but it can be inferred that groundwater flux is controlled by hydraulic properties and that the temperature response is strongly sensitive to that flux. Detailed quantitative interpretation is needed to support this conclusion.

Planned future work includes laboratory work on soil samples to constrain hydraulic and thermal properties, proper verification and calibration of temperature data from the fiber optics, hydraulic testing in an observation well as well as numerical modelling of Site B where the repeatability tests were done.

Acknowledgments

The fieldwork and research undertaken in this paper would not have been possible without the collaboration of personnel from Université de Rennes I and INRS. Thanks are given to the Université de Rennes I team: Nataline Simon, Jérôme de la Bernadie and Bezhad Pouladi for their expertise and guidance on the use of fiber optics.

From INRS, thanks are due to Jean-Marc Ballard for his help in coordinating the fieldwork, as well as all those who helped during the field experiments: Maria Isabel Velez Marquez, Violaine Gascuel, Jasmin Raymond, Marie-Pierre Champagne, Julie Domaine, Elise Comeau and Jean-Sebastien Gosselin.

This work is part of the ANR project EQUIPEX CRITEX (grant ANR-11-EQPX-0011), and the LIA France-Québec RESO "REssources et SOciétés" from which it has been supported.

References

Anderson MP (2005) Heat as a ground water tracer. *Groundwater* 43(6): 951-968.

Bakker M, Caljé R, Schaars F, van der Made KJ & de Haas S (2015) An active heat tracer experiment to determine groundwater velocities using fiber optic cables installed with direct push equipment. *Water Resources Research* 51(4): 2760-2772.

Bense V, Read T, Bour O, Le Borgne T, Coleman T, Krause S, Chalari A, Mondanos M, Ciocca F & Selker J (2016) Distributed Temperature Sensing as a downhole tool in hydrogeology. *Water Resources Research* 52(12): 9259-9273.

des Tombe BF, Bakker M, Smits F, Schaars F & van der Made K-J (2019) Estimation of the variation in specific discharge over large depth using Distributed Temperature Sensing (DTS) measurements of the heat pulse response. *Water Resources Research* 55(1):811-826.

Fauveau, E (2006). *Caractérisation hydrogéologique et identification de faciès des dépôts meubles par enfoncement direct et forage par rotopercussion*. M.Sc. thesis, Université du Québec, Institut national de la recherche scientifique, Québec, 170 p.

Ouellon T, Lefebvre R, Marcotte D, Boutin A, Blais V & Parent M (2008) Hydraulic conductivity heterogeneity of a local deltaic aquifer system from the kriged 3D distribution of hydrofacies from borehole logs, Valcartier, Canada. *Journal of Hydrology* 351: 71-86.

Ouellon T, Lefebvre R, Blais V, Racine C & Ballard JM (2010). Synthèse du contexte hydrogéologique et de la problématique du TCE dans le secteur Valcartier, Québec, Canada. Research report R-961, INRS, *Centre - Eau Terre Environnement*, ISBN 978-2-89146-560-1, 119 p.

Selker JS, Thevenaz L, Huwald H, Mallet A, Luxemburg W, de Giesen NV, Stejskal M, Zeman J, Westhoff M & Parlange MB (2006) Distributed fiber-optic temperature sensing for hydrologic systems. *Water Resources Research* 42(12): 8.

Field testing of a standing column well located in the Nicolet formation

Gabrielle Beaudry[1], Philippe Pasquier[1], Denis Marcotte[1]

[1]Polytechnique Montreal, Genies civil, geologique et des mines, Montreal, Canada

gabrielle.beaudry@polymtl.ca

DOI : https://doi.org/10.5281/zenodo.3565977

Keywords: Standing column well, groundwater, bleed, thermal response test

Abstract

A dynamic thermal response test is conducted on an experimental standing column well located in the Nicolet Formation to evaluate the impact of bleed on its thermal performance. Results suggest that a bleed rate of 7.5 L/min increases the apparent thermal conductivity by 2.5 times compared with a no-bleed scenario.

1. Introduction

Standing column wells (SCW) are efficient ground heat exchangers that rely on the recirculation of groundwater in a deep and uncased borehole. "Bleeding" the Well (discharging a small amount of groundwater) has been identified as a key feature of SCWs performance. The capacity to bleed the Well can however be limited in areas with a low bedrock hydraulic conductivity. The objective of this short paper is to evaluate the influence of a realistic bleed operation on the thermal performance of an experimental SCW located in the Nicolet Formation.

2. Methods and techniques

A thermal response test is conducted on an experimental system made of a 215-m-deep SCW and a 15o-m-deep injection well. The latter allows reinjection of the bleed water. Groundwater is recirculated in the SCW at a rate of 75 L/min for 18 days. Two 4-day heating phases are carried out using a 24-kW water heater. Bleed rate is o L/min during phase 1, and 7.5 L/min (1o% of the total pumping rate) during phase 2. Note that bleed rate cannot be further increased without overflowing the injection Well due to the low bedrock hydraulic conductivity that is 5.7e-7 m/s (Beaudry et al. 2o19). Temperatures at the SCW's inlet and outlet are monitored and the apparent thermal conductivity for both phases is computed using the infinite line source theory (Mogensen 1983).

3. Results

The apparent thermal conductivity measured for the first heating phase of the test involving no bleed is 2.42 W/mK, whereas it is 6.11 W/mK for the second heating phase involving a 7.5 L/min bleed. The mean temperature evolution during the test is shown in Fig. 1.

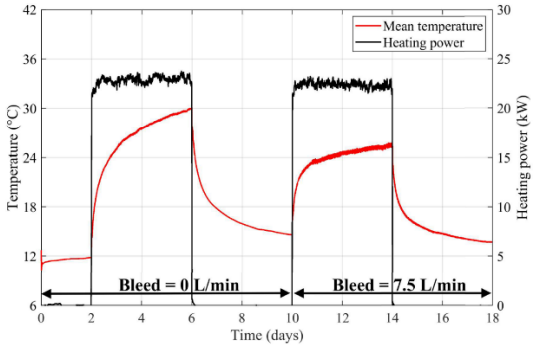

Fig. 1 Inlet - outlet mean temperature during the test.

4. Discussion

Visual inspection of the results shows that discharging 7.5 L/min tempers the temperature variation inside the SCW. This enhanced thermal efficiency translates as an apparent thermal conductivity value that is 2.5 times higher than in the no-bleed scenario. These results are mostly attributable to the stimulation of advective heat transfer when bleed acts as a net pumping rate, which creates a drawdown and promotes renewal of the well's water content.

5. Conclusions

It was demonstrated in this study that discharging 7.5 L/min (1o% ratio) enhances heat transfer around an experimental SCW and increases the apparent thermal conductivity by about 2.5 times. These findings suggest that bleed remains a key feature of SCW operation even if the system is located in a hydrogeological unit characterized by a low bedrock hydraulic conductivity such as the Nicolet Formation.

References

Beaudry G., Pasquier P. and Marcotte D. (2019), "The impact of rock fracturing and pump intake location on the thermal recovery of a standing column well: model development, experimental validation, and numerical analysis", Science and technology for the built environment, 25: 8, p. 1052-1068.

Mogensen P. (1983), "Fluid to duct wall heat transfer in duct system heat storages", Document-Swedish Council for Building Research, p.652-657.

Large-scale landslides hiding the geothermal potential of San Agustín del Maíz geothermal field, México

Jorge Alejandro Guevara-Alday[1,4], Víctor Hugo Garduño-Monroy[2,4] †, Emanuel Olvera-García[3,4], Sergio Manuel Nájera-Blas[4], Mikhail Ostrooumov[2], Alain Tremblay[1]

[1]University of Quebec in Montreal, Department of Earth and Atmospheric sciences H2X3Y7, Montreal, Canada
[2]Michoacán University of "San Nicolas de Hidalgo", Research Institute in Earth Sciences, 58060 Morelia, Mexico
[3]University of Bari "Aldo Moro", Department of Earth and Geoenvironmental, 70125 Bari, Italy
[4]Mexican Center of Innovation in Geothermal Energy (CeMIEGeo), 22860 Ensenada, México
aguevaraalday@gmail.com

DOI: https://doi.org/10.5281/zenodo.3565980

Keywords: Slope stability, tectonic active, medium enthalpy, sinter deposits

Abstract

Large-scale landslides are usually linked to fault ruptures in active tectonic settings, most of the time in step slopes landscapes. San Agustín del Maíz geothermal field is located within the Cuitzeo basin at the central sector of the Trans-Mexican Volcanic Belt (TMVB), where thanks to remote sensing and fieldwork were recognized five hills formed by landslides covering part of the geothermal upwelling, these landslides are made up mainly by broken fragments of pyroclastic deposits and andesites from the surroundings rocks which are hydrothermal altered and contain veins made of calcite, quartz, chlorite and opal crystals.

1. Introduction

Commonly large-scale landslides are triggered by a wide number of factors, including anomalous rainfalls, rapid snow melts, volcanic eruption (Cruden and Varnes, 1996). Although, within continental volcanic belts characterized by active tectonics, landslides are frequently triggered by earthquakes or swarms of them (Evans et al., 1987; Schuster et. al.,1992).

The study area is located in the Cuitzeo tectonic basin, in the central part of the TMVB (Demant 1978). This volcanic province dates back to the middle to late Miocene (Ferrari et. al. 1999) and derives from the subduction of the Cocos plate under the North American plate along the Pacific trencher (Demant 1978) (**Fig. 1a**). The evidences of geothermal activity located on the south shore of Cuitzeo Lake are: thermal pools, mug volcanos, fossil and current sinter deposits which follow NE – SW and NW – SE trends and reach temperatures up to 94 °C.

2. Methods and techniques

A morpho-structural analysis was performed using 5 m resolution LIDAR (Laser Imagen Detection and Ranging) and complemented by using orthophotos and aerial photographs products of National Institute of Statistic and Geographic (INEGI by its acronym in Spanish). Then were carried out structural stations along fault traces and dots around the allochthonous bodies by classic field mapping and stratigraphic sections.

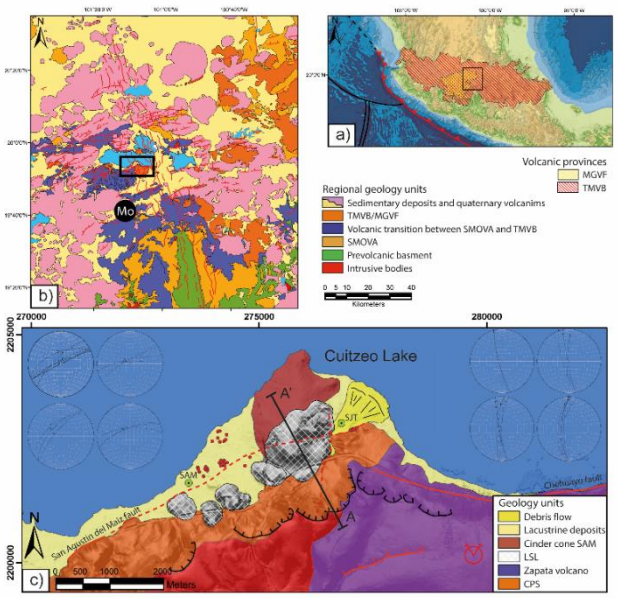

Fig. 1 a) Geodinamic context of the Tran-Mexican Volcanic Belt (TMVB) and the Michoacan-Guanajuato Volcanic Field (MGVF), the black box represents the area enlarged in b; b) geological map illustrating the geological evolution since Mesozoic until today, the black box shows the detail area enlarged in c; c) synthetic geological map of the interest area which shows the main lithologies across, showing the distribution of fossil and current thermal manifestations in red dots and the depletion zones identified along San Agustin del Maíz fault scarp. The major abbreviations are Mo: Morelia; SMOVA: Sierra Madre Oriental Volcanic Belt.

3. Results

The geological sequence of the study area consist of: a well fractured andesite sequence named Mil Cumbres Andesite (MC) of 21.5 Ma at the bottom, followed by a ~140 m of pyroclastic deposits package named Cuitzeo Pyroclastic Sequence (CPS) expose mainly along the ENE – WSW fault scarp (Fig 1c) and with evidences of hydrothermal alteration in the middle and at the bottom of the slope, overlaying this sequences there are the first evidences of monogenic activity from Tarímbaro sequences of <18.6 Ma, which is part of the Michoacán Guanajuato Volcanic Field (MGVF). The entire sequence is tilting 32° southward due to ENE – WSW striking listric faults, dipping toward NW (**Fig 2h**). The top of the lithological sequence is crowed by Lacustrine Deposits of Cuitzeo Lake (LD), filling the tectonic basin (**Fig 2a**). Particularly important are some outcrops at El Caido (the biggest landslide) that exhibit evidences of fossil hydrothermal activity, filling with calcite ± chloride ± quartz and structural attitude unlike (**Fig. 2h**) of the units located south along the fault scarp, also important are some small outcrops with stockwork structures (**Fig. 2i**).

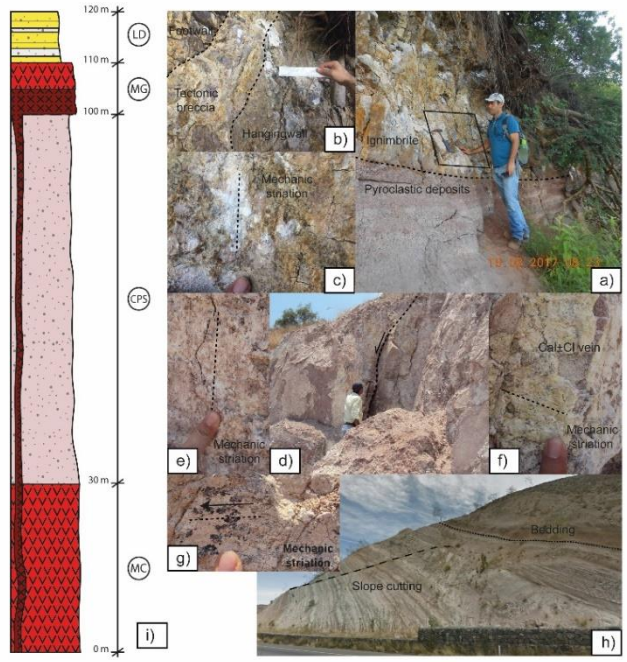

Fig. 2 a) Geological map that illustrate the principal sequences in the research area,; b) San Agustin del Maíz fault plane where was identified a tectonic breccia enlarged in c) and slickensides in secondary mineralization d); e) Damage zone next to SJT that exhibit a uncountable number of fault planes which are strike slip and oblique faults striking N – S often filling by Cal±Cl such as f) and h) and normal fault striking NE – SW like h); i) Outcrop of pyroclastic sequences tilted 32°; j) Stratigraphic column type along San Agustin del Maíz fault scarp is made up: MC: Mil Cumbres Andesite; CPS Cuitzeo Pyroclastic Sequence; MG: Michoacán Guanajuato Volcanic Field and LC: Lacustrine Deposits of Cuitzeo.

After the analysis of fault populations were recognize two different fault sets: 1) Normal faults striking ENE – WSW and dipping NW with lateral component (both right and left) (Fig. 1c); controlling the morphology of the region and acting as rise pathways for hydrothermal fluids in San Agustin geothermal field. 2) Right lateral strike slip and oblique faults striking from NNW – SSE to NNE-SSW (Fig. 1c) were defined as a fault zone located between San Agustin del Maíz (SAM) and San Juan Tararameo (SJT). Based on its position between two normal faults it is considered as a transfer zone between San Agustin del Maíz and Chehuayo faults.

4. Discussion

Although depletion zones are not present across the area in the most cases probably because weathering, some evidences over the principal slope NE – SW trend such as concave crowns forward the slipping direction (Fig. 1c) and the internal structure of every large-scale landslide on Cuitzeo basing like random tilting (**Fig. 3a, 3e**), classified them how rotational landslides. With respect of their role as caprock of a geothermal field, it is well known slip surface could be affected by weathering developing a clay layer that acts how an impermeable surface allowing a reactivation of the body (Rotaru et. al. 2007). Keeping this in mind, clay layers may also act how a fluid boundary in both senses downward and upward, cutting off the rise of hydrothermal fluids through it.

5. Conclusions

The Miocenic tectonic activity has performed an important role since the first stages of TMVB up to date controlling the volcanic activity, morphology and even extension thought tectonics basins like Cuitzeo Lake. Paleo seismic and recent records of this constant tectonic activity proved not only its potential seismic hazard to cities but its high potentially as trigger of large-scale landslides such as they founded on Cuitzeo basin.

Acknowledgments

This work was supported by the Mexican Center of Innovation in Geothermal Energy (CEMiEGeo) as part of the grant "Fondo Sectorial CONACYT-SENER Sustentabilidad Energetica UMSNH-CeMIEGeo P17.

References

Cruden D. M. y Varnes D. J. (1996), 'Landslides types and processes", in Turner, A. K. y R. L. Schuster (eds.), Landslides: Investigation and Mitigation. Washington D.C., National Academy of Science.

Demant, A., 1978, Características del eje Neovolcánico Transmexicano y sus problemas de interpretación: Universidad Nacional Autónoma de México. Instituto de Geología. 2 (2), 172-187.

Evans, S. G., Aitken, J. D.,Wetmiller, R. J., and Horner, R. B., 1987, A rock avalanche triggered by the October 1985 North

Nahami earthquake, District of Mackenzie, N.W.T.: Canadian Journal of Earth Sciences, v. 24, p. 176–184.

Ferrari, L., Lopez-Martinez, M., Aguirre-Diaz, G., Carrasco-Nunez, G., 1999. Space-time pat- terns of Cenozoic arc volcanism in central Mexico: from the Sierra Madre Occidental to the Mexican Volcanic Belt. Geology 27 (4):303–306. http://dx.doi.org/10.1130/ 0091-7613(1999)027<0303:Stpoca>2.3.Co;2

Rotaru, A., Oajdea, D., & Răileanu, P. (2007). Analysis of the landslide movements. International Journal of Geology, 1(3), 70-79

Sensitivities of thermal anomalies from high thermal conductivity formations in the Williston basin

Kayla R. Moore[1], Hartmut M. Holländer[1]

[1.] University of Manitoba, Department of Civil Engineering, Winnipeg, Canada
ummoor37@myumanitoba.ca

DOI: https://doi.org/10.5281/zenodo.3565988

Keywords: power, temperature, halite, dolomite, thermal conductivity

Abstract

A numerical model case-study in the Williston Basin was used to investigate thermal anomalies at the top of high thermal conductivity formations. In the Williston Basin, a thick Devonian halite formation, the Prairie Evaporite, is underlain by dolomite formations, and both have high thermal conductivities. The temperature at the bottom of the production well was sensitive to site-specific ranges in thermal conductivities of 2.8 to 5.1 W m^{-1} $°C^{-1}$, boundary temperatures of 98 to 154°C, and formation thicknesses of 385 to 534 m. Temperatures were calculated at 86 to 135°C at the top of the Prairie Evaporite.

1. Introduction

Heat in sedimentary basins is primarily transmitted by conduction. Minerals such as halite and dolomite have thermal conductivities 2 to 4 times higher than other sedimentary rocks (Grasby et al., 2012). The objective was to quantify the sensitivities of the magnitude of the thermal anomaly for a geothermal system targeting the Prairie Evaporite formation and underlying dolomite formations in the Williston Basin, Saskatchewan (**Fig. 1**).

eriod	Formation	Thick. (m)
evonian	Prairie Evap.	130±29
	Winnipegosis	42±27
ilurian	Ashern	16±4
	Interlake	191±12
	Stonewall	30±1
	Stony Mtn.	36±2
	Red River	135±5

Fig. 1 Location of the study area in the Williston Basin and thicknesses of targeted formations.

2. Methods and techniques

A numerical model was used to investigate heat flow in the Prairie Evaporite, depth to top 2525 m, and underlying dolomite formations (**Fig. 1**) using estimated ranges for thermal conductivity (Firoozy, 2016), thicknesses (TGI Williston Basin Working Group, 2008) and temperature at the top of the Red River formation (Manz, 2011). The finite element code FEFLOW (Diersch, 2014) was used to complete the heat flow analysis.

3. Results and Discussion

Table 1 Temperatures at the top of the Prairie Evaporite with varying heat flow parameters.

Thermal Cond. (W m^{-1} $°C^{-1}$)	Boundary Temp (°C)	Thickness (m)	Prairie Temp (°C)
3.9	*126*	*460*	*111*
5.1	*126*	*460*	*114*
2.8	*126*	*460*	*106*
3.9	*154*	*460*	*135*
3.9	*98*	*460*	*86*
3.9	*126*	*534*	*109*
3.9	*126*	*385*	*113*

Drilling depths can be reduced in sedimentary basins by targeting high thermal conductivity formations, which result in warm temperature anomalies (**Table 1**). However, the temperature boundary at the top of the Red River had the greatest influence on temperature at the top of the Prairie Evaporite. Increased formation thickness resulted in decreased temperature in the Prairie Evaporite at the same Red River temperature boundary.

4. Conclusions

Modeled study area temperatures at the top of the Prairie Evaporite ranged from 86 to 135°C and were sensitive to thermal conductivity, underlying temperatures, and formation thickness.

Acknowledgments Thanks to the U of M URGP and Vanier CGS.

References

Grasby, S. E., Allen, D. M., Bell, S., et al. (2012). "Geothermal Energy Resource Potential of Canada" Vol. Open File 6914, Geological Survey of Canada, Calgary, AB.

Firoozy, N. (2016). "Assessment of Geothermal Application for Electricity Production from the Prairie Evaporite Formation of Williston Basin in South-West Manitoba" (Master of Science), University of Manitoba, Winnipeg, Manitoba.

TGI Williston Basin Working Group. (2008). "Devonian Prairie Evaporite: isopach" Manitoba Science, Technology, Energy and Mines; Manitoba Geological Survey, Winnipeg, MB

Manz, L. A. (2011). "Deep Geothermal Resources: Estimated Temperatures on Top of the Red River Formation Kenmare 100K Sheet, North Dakota" North Dakota Geological Survey, Bismark, ND

Diersch, H. (2014). "FEFLOW Finite Element Modeling of Flow, Mass and Heat Transport in Porous and Fractured Media", Springer, New York.

Impact of the operation of a standing column well on clogging and scaling

Léo Cerclet[1], Benoît Courcelles[1], Philippe Pasquier[1]

[1.] Polytechnique Montréal, Department of Civil, Geological and Mining Engineering, P.O. Box 6079 Centre-Ville, Montréal, Québec, Canada H3C 3A7)
leo.cerclet@polymtl.ca

DOI: https://doi.org/10.5281/zenodo.3565991

Keywords: Scaling; Clogging; Geothermal open-loop systems; Standing Column Wells

Abstract

A Standing Column Well (SCW) is a low-temperature geothermal system that shows a great potential to reduce greenhouse gases emissions. In a SCW, groundwater is continuously recirculated in an uncased well, bringing the water in direct contact with the rock. Since the physico-chemistry of groundwater is modified by the operation, this new equilibrium can be prone to clogging. The work achieved so far shows a direct link between the operation of a SCW and the load of calcium. Our results indicate that on/off submersible pump sequences create ideal conditions for precipitation in geothermal equipments, such as heat exchangers.

1. Introduction

SCWs demonstrate high heat exchange rate (Orio et al. 2005) and represent a promising solution among the available ground heat exchangers. It can reduce the capital cost compared to closed-loop systems (Lee 2009; O'Neil et al. 2006). SCWs can be installed in small areas such as dense urban zones (Pasquier et al. 2016). In a SCW, groundwater is continuously recirculated in an uncased well, bringing the water in direct contact with the rock. Since groundwater is being mixed, oxygenated, and warmed or cooled, the well and the mechanical equipments can be prone to clogging and scaling (Rafferty 2004), which can impact the long-term performance and maintenance costs of the system. More specifically, calcium carbonate scaling and iron-related fouling are the most common water quality problems (Rafferty 2004; Park et al. 2015). In the Montreal area, the substratum is composed of carbonate sedimentary rocks, which can lead to calcium carbonate precipitation during SCW operation. Although current literature identifies the main causes of clogging, the impact of the operation strategy of a SCW has yet not been investigated.

2. Methods and techniques

The chemical signature of groundwater and the operation parameters of an experimental SCW were monitored during a one-year period through the use of a geothermal mobile unit. This unit contains four heat pumps, a heat exchanger, monitoring devices and a water treatment unit that can treat a fraction of the total flow.

3. Results

The work achieved so far shows a direct link between the operation of a SCW and the concentration of calcium in groundwater. More specifically, our results indicate that on/off sequences create ideal conditions for increase of calcium content in the groundwater. After two years of operation and 13 involuntary on/off sequences, two flow sensors were cleaned (**Fig. 1**). This operation has permitted to sample the deposit on the pipe. It was analyzed with a scanning electron microscope (SEM). The results show that this deposit is higher concentrated in calcium, oxygen and carbon than other chemical elements.

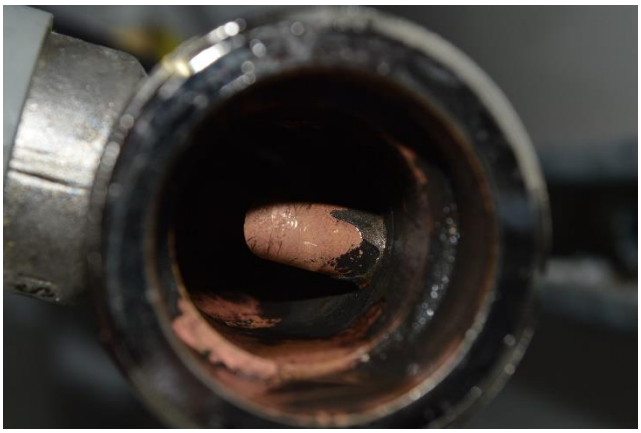

Fig. 1 Picture of a flow meter, where it is possible to observe depositions after two years of operation.

4. Discussion

Our observations showed that on/off sequences create ideal conditions for groundwater to dissolve the rock, i.e. increase the geochemical load. The direct consequence of this observation is the potential precipitation in mechanical equipments. Indeed, the temperature increase generated by equilibrium with the warm laboratory as well as water stagnation creates optimal conditions for calcite precipitation.

5. Conclusions

The study has demonstrated the impact of the operation of a SCW that can lead to the precipitation of a thin layer of calcium carbonates. Nevertheless, after two years of operation, the effect of precipitation is limited to a couple of monitoring devices (i.e. flow meters) and do not affect the entire system.

References

Lee, J. Y. (2009). Current status of ground source heat pumps in Korea. Renewable and Sustainable Energy Reviews, 13(6-7), 1560-1568.

O'Neill, Z. D., Spitler, J. D., & Rees, S. (2006). Performance analysis of standing column well ground heat exchanger systems. ASHRAE transactions, 112(2), 633-644.

Orio, C. D., Chiasson, A., Johnson, C. N., Deng, Z., Rees, S. J., & Spitler, J. D. (2005). A Survey of Standing Column Well Installations in North America. ASHRAE transactions, 111(2).

Pasquier, P., Nguyen, A., Eppner, F., Marcotte, D., & Baudron, P. (2016). Standing column wells. In Advances in Ground-Source Heat Pump Systems (pp. 269-294). Woodhead Publishing.

Park, Y., Kim, N., & Lee, J. Y. (2015). Geochemical properties of groundwater affected by open loop geothermal heat pump systems in Korea. Geosciences Journal, 19(3), 515-526.

Rafferty, K. D. (2004). Water chemistry issues in geothermal heat pump systems. Ashrae Transactions, 110, 550.

Effect of temperature-dependent thermal conductivity on the temperature field at depth: case study of Kuujjuaq, Canada

Mafalda M. Miranda[1,2], Maria Isabel Vélez[1], Jasmin Raymond[1,2]

[1.] INRS – Institut national de la recherche scientifique, Centre Eau Terre Environnement, Québec City, Canada
[2.] CEN – Centre d'études nordiques, Université Laval, Québec City, Canada
mafalda_alexandra.miranda@ete.inrs.ca

DOI: https://doi.org/10.5281/zenodo.3565995

Keywords: geothermal energy, thermal properties, empirical equations, numerical model, Nunavik

Abstract

This work aims at assessing the influence of temperature-dependent thermal conductivity on the temperature distribution at depth. Thermal conductivity was evaluated at temperatures ranging from 20 to 160 °C. The experimental results were implemented in COMSOL Multiphysics to simulate the temperature at depth. The data was implemented as analytical and interpolation functions. The results reveal that the analytical functions lead to a 11 % increase of the temperature at 5 km. In turn, COMSOL's interpolation function shows an increase of about 9.5 %. This new evaluation predicts temperatures of 105 to 113 °C at 5 km below Kuujjuaq (Canada).

1. Introduction

Thermal conductivity is temperature-dependent, decreasing with the increase of the later (e.g., Clauser and Huenges et al. 1995). Several empirical relationships have been proposed in the literature to describe this behavior (e.g., Lee and Deming 1998). In this work, thermal conductivity was evaluated at temperatures of 20 to 160 °C and the results fit to literature functions using the obtained experimental coefficients. The empirical equations were implemented in a finite element model as analytical functions to infer the temperature at depth with heat conduction simulations. The results obtained from the laboratory were additionally implemented as interpolation function. This allowed to quantify the influence of the different functions on the numerical simulation of the temperature at depth.

2. Methods

A total of 9 samples were used to evaluate thermal conductivity at temperatures ranging from 20 to 160 °C. The dataset comprises 4 paragneiss samples and 5 diorite samples, the main lithologies outcropping nearby Kuujjuaq's community (QC, Canada; **Fig. 1**).

The instrument used to evaluate thermal conductivity is the FOX50 Heat Flow Meter (Raymond et al. 2017). The analysis is made when temperature across the sample reaches steady state. A temperature difference is imposed on both plates and successive data acquisition cycles are run until the temperature of the upper and lower plates and transducer signals satisfy the equilibrium criteria to declare the sample in thermal equilibrium. Then, thermal conductivity is evaluated. Each plate must meet each equilibrium criterion independently. These criteria are: 1) temperature equilibrium (TE) criterion, 2) semi-equilibrium (SE) criterion, 3) percent equilibrium (PE) criterion, 4) number of blocks of PE, and 5) inflexion criterion. The accuracy of the thermal conductivity evaluation with this instrument is about 3 %.

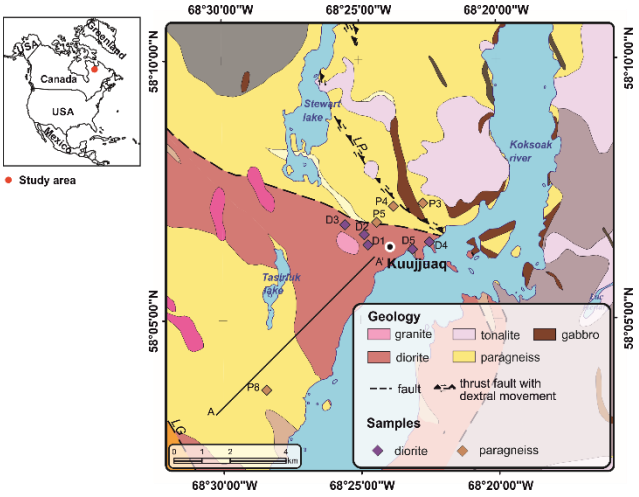

Fig. 1 Geographical and geological setting (adapted from SIGÉOM 2019)

The results were fit to the following relationships:

$$\frac{1}{\lambda(T)} = \frac{1}{\lambda_{20}} + aT \quad (1)$$

$$\lambda(T) = \frac{\lambda_{20}}{1 + b(T - 20)} \quad (2)$$

where λ (W m^{-1} K^{-1}) is thermal conductivity, T (°C) stands for temperature and a and b are experimental coefficients controling the temperature dependence of the thermal conductivity.

The 2D steady state temperature field at depth was simulated numerically using COMSOL Multiphysics with a finite element approach to solve heat conduction in the crust. The temperature distribution was modeled for a rectangular geometry with a width of 8 km and a depth of 10 km. The center of the 2D model corresponds to a change in lithology between paragneiss and diorite (**Fig. 1**). A constant surface temperature of -1 °C and a constant heat flux of 35.5 mW m^{-2} were set as upper and lower boundary conditions. Further details on the modeling approach are given in Miranda et al. (unpublished). The temperature dependence of thermal conductivity was implemented in the materials as both analytical and interpolation functions. The internal heat generation from radioactive element decay was assumed constant and dependent of the material.

3. Results and discussion

Thermal conductivity as a function of temperature reveals a decrease of more than 40 % (**Table 1**).

Table 1 Thermal conductivity as a function of temperature

T (°C)	λ (W m^{-1} K^{-1})	
	Paragneiss (n = 4)	Diorite (n = 5)
20	2.32	2.39
40	2.28	2.33
60	2.22	2.25
80	2.11	2.10
100	2.05	1.96
120	1.95	1.86
140	1.88	1.78
160	1.63	1.49
Variation ratio	-42 %	-60 %

n – number of samples

Using a constant thermal conductivity, independent of temperature, to simulate the temperature field at depth, a value of about 90 °C is obtained at 5 km depth (**Fig. 2a**). However, if Eq. (1) and (2) are implemented in COMSOL, the temperature at 5 km increases to 113 °C and 107 °C, respectively (**Fig. 2b, c**). Using COMSOL's interpolation function leads to a temperature of 105 °C at 5 km depth (**Fig. 2d**).

Temperature-dependent thermal conductivity leads to an increase on the temperature field at depth. An observation that agrees with the works of Lemenager et al. (2018) and Vélez et al. (2018). The difference between the non-temperature-dependent and temperature-dependent thermal model is up to 12 %. Applying COMSOL's interpolation function, the difference between both models is 9.5 %. A difference of 12 and 10 % is found by implementing Eqs. (1) and (2) as analytical functions.

There is still a high uncertainty due to the lack of deep temperature measurements in Kuujjuak. Nevertheless, this new evaluation of the temperature field below Kuujjuaq indicates potential use of the geothermal resources for direct space heating.

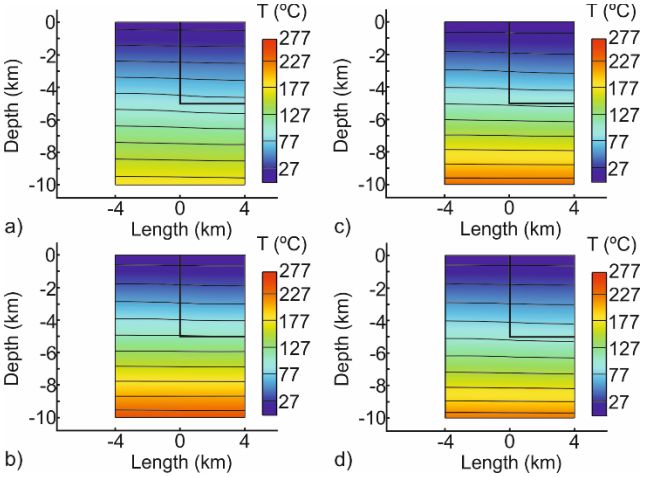

Fig. 2 2D temperature distribution simulated below Kuujjuaq. a) constant and b) to d) temperature-dependent thermal conductivity

4. Conclusions

Thermal conductivity decreases as a function of increasing temperature. This has an influence on the evaluation of the temperature distribution at depth. A non-temperature-dependent model suggests a temperature of 100 °C at 5 km depth. This value increases up to 113 ° C for a temperature-dependent model. The different relationships to describe the behavior of thermal conductivity as a function of temperature are observed to have an influence on the simulation results.

This new evaluation of the temperature field below Kuujjuaq predicts suitable temperatures to directly use the deep geothermal resources. Space heating might be a viable option to offset the diesel consumption and provide energy security to the communities north of the 49° parallel in the context of Nunavik.

Acknowledgments

This study was funded by the *Institut Nordique du Québec* (INQ) through the *Chaire de recherche sur le potential géothermique du Nord* awarded to Jasmin Raymond. The *Centre d'études nordiques* (CEN), supported by the *Fonds de recherche du Québec – nature et technologies* (FRQNT), and the *Observatoire Homme Milieu Nunavik* (OHMI) are further acknowledged for helping with field campaigns cost and logistics.

References

Clauser, C., Huenges, E. (1995), "Thermal conductivity of rocks and minerals", in Ahrens, T.J. (editor), Rock Physics & Phase Relations: A Handbook of Physical Constants, AGU, pp. 105-126

Lemenager, A., O'Neill, C., Zhang, S., Evans, M. (2018), "The effect of temperature-dependent thermal conductivity on the geothermal structure of the Sydney Basin", Geothermal Energy, 6:6, 2-27

Raymond J., Comeau F-A., Malo M., Blessent D., Sánchez I.J.L. (2017), "The Geothermal Open Laboratory: a free space to measure thermal and hydraulic properties of geological materials", presented at IGCP636 Annual Meeting, Santiago de Chile, 2017 Nov 21

SIGÉOM (2019), « Système d'information géominière du Québec; Carte Interactive ». http://sigeom.mines.gouv.qc.ca. Accessed on 18 September 2019

Vélez, M. I., Blessent D., Córdoba, S., López-Sanchez, J., Raymond, J., Parra-Palacio, E. (2018), "Geothermal potential assessment of the Nevado del Ruiz volcano based on rock thermal conductivity measurements and numerical modeling of heat transfer", J S Am Earth Sci, 81, 153-164

Effect of confining pressure on porosity and thermal conductivity: an example from crystalline rocks of Kuujjuaq, Canada

Mafalda M. Miranda[1,2], Inès Kanzari[1], Jasmin Raymond[1,2]
[1.] INRS – Institut national de la recherche scientifique, Centre Eau Terre Environnement, Québec City, Canada
[2.] CEN – Centre d'études nordiques, Université Laval, Québec City, Canada
mafalda_alexandra.miranda@ete.inrs.ca

DOI: https://doi.org/10.5281/zenodo.3565997

Keywords: energy, geothermal, laboratory analyses, empirical equation, Nunavik

Abstract

The aim of this work is to obtain an experimental relationship that best describes the effect of confining pressure on primary porosity, and indirectly evaluate the influence of confining pressure on thermal conductivity. The results reveal that primary porosity decreases logarithmically as a function of confining pressure. For the pressure range 2.8 to 48.3 MPa, thermal conductivity indirectly evaluated increases less than 10 %. Considering the effect of confining pressure and temperature on thermal conductivity, a temperature of 104 °C at 5 km is simulated below Kuujjuaq (QC, Canada).

1. Introduction

The application of pressure on a rock sample leads to compression of the interstitial pore spaces (e.g., Hui-yuan et al. 2016) and, consequently, to a decrease of the primary porosity. This, in turn, causes an increase in the thermal conductivity of the geological materials.

In the present work, the primary porosity of rock samples was evaluated at confining pressures ranging from 2.8 to 48.3 MPa. Then, the effect of confining pressure on thermal conductivity was indirectly inferred considering the relationship between porosity and thermal conductivity.

2. Methods

Primary porosity of 24 crystalline rock samples was evaluated by a combined gas permeameter-porosimeter AP-608 from Core Test (e.g., Raymond et al. 2017). The analyses follow Boyle's law. This law states that the pressure exerted by a given mass of an ideal gas is inversely proportional to the volume it occupies (Raymond et al. 2017 and references therein). This instrument can evaluate the hydraulic properties at confining pressures ranging from 2.8 to 68.9 MPa.

Following the evaluation of porosity at different confining pressures, the results were fit to the following functions:

$$\phi(Pc) = \phi_0 + aPc \quad (1)$$

$$\phi(Pc) = \phi_0 Pc^{-a} \quad (2)$$

$$\phi(Pc) = \phi_0 \exp^{-aPc} \quad (3)$$

$$\phi(Pc) = a\ln(Pc) + \phi_0 \quad (4)$$

where Φ (%) is primary porosity, Pc ($\times 10^6$ Pa) is confining pressure and a ($\times 10^6$ Pa^{-1}) is an experimental coefficient that controls the confining pressure dependence of the porosity. The subscript 0 stands for porosity at ambient pressure conditions (1 atm = 0.1 MPa).

The following mixing models were used to describe the relationship between thermal conductivity and porosity:

$$\lambda_{bulk} = \phi\lambda_{fluid} + (1-\phi)\lambda_{solid} \quad (5)$$

$$\frac{1}{\lambda_{bulk}} = \frac{\phi}{\lambda_{fluid}} + \frac{(1-\phi)}{\lambda_{solid}} \quad (6)$$

$$\lambda_{bulk} = \lambda_{fluid}^{\phi} \times \lambda_{solid}^{(1-\phi)} \quad (7)$$

where λ (W m^{-1} K^{-1}) is thermal conductivity. The subscripts *bulk*, *fluid* and *solid* stand for the bulk thermal conductivity, the thermal conductivity of the fluid phase filling the pores, and the thermal conductivity of the solid phase, respectively. Considering the previous relationships, the effect of confining pressure on thermal conductivity is indirectly inferred.

3. Results

The results reveal a decrease of primary porosity with the increasing confining pressure. On average, the primary porosity decreases more than 50 % for all the lithologies analyzed (**Table 1**). These results were fit to Eqs. (1) to (4) and the best-fit is given by the logarithmic function (**Fig. 1**), with a coefficient of determination (R^2) varying from 0.98 to 1.00.

Paragneiss:

$$\phi(Pc) = -0.5\ln(Pc) + 2.81 \quad (8)$$

Diorite-gabbro:

$$\phi(Pc) = -0.3\ln(Pc) + 2.05 \quad (9)$$

Table 1 Porosity as a function of confining pressure and depth

Pc (×10⁶ Pa)	Φ (%)		
	Paragneiss (n = 8)	Diorite-gabbro (n = 9)	Tonalite-granite (n = 7)
2.8	2.25	1.62	2.07
4.8	2.11	1.56	1.95
6.2	1.99	1.48	1.83
10.3	1.71	1.31	1.61
20.7	1.36	1.04	1.31
34.5	1.12	0.86	1.12
48.3	0.94	0.72	0.97
Variation ratio	58 %	56 %	53 %

n – number of samples

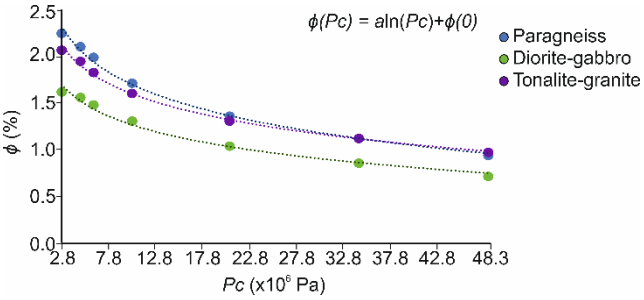

Fig. 1 Porosity as a function of confining pressure

Tonalite-granite:

$$\phi(Pc) = -0.4\ln(Pc) + 2.53 \quad (10)$$

Considering the geometric mean to describe the relationship between thermal conductivity and porosity, then, by integration of Eq. (4) in Eq. (7), a general function is obtained to indirectly infer the effect of confining pressure on thermal conductivity:

$$\lambda_{bulk} = \lambda_{fluid}^{\left[a\ln(Pc)+\phi_0\right]} \times \lambda_{solid}^{\left(1-\left[a\ln(Pc)+\phi_0\right]\right)} \quad (11)$$

The results reveal a less than 10 % increase of thermal conductivity for the confining pressure range of 2.8 to 48.3 MPa (**Fig. 2**).

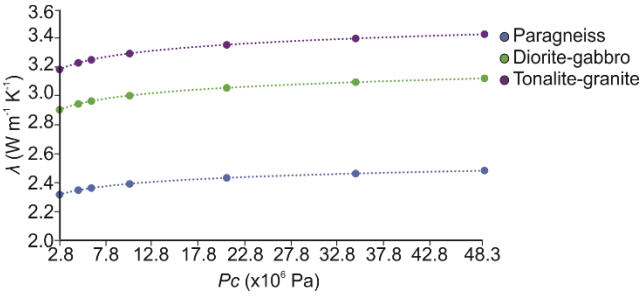

Fig. 2 Thermal conductivity as a function of confining pressure

The relationship between thermal conductivity and confining pressure was implemented in a finite element COMSOL Multiphysics model as an interpolation function to simulate heat conduction in the crust.

The results reveal that at 5 km, a temperature of 80 °C is expected to be find below Kuujjuaq (**Fig. 3b**). Neglecting the effect of confining pressure, the temperature at 5 km is predicted to be 90 °C (**Fig. 3a**).

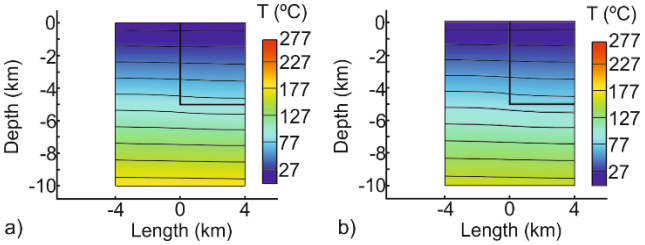

Fig. 3 2D temperature distribution simulated below Kuujjuaq (see Miranda et al. (this volume) for further details on the numerical model). a) constant and b) pressure-dependent thermal conductivity

In turn, if the temperature and confining pressure dependence on thermal conductivity are considered, the temperature simulated below Kuujjuaq increases by 9 %. In this case, a temperature of 104 °C is predicted at 5 km depth (**Fig. 4**)

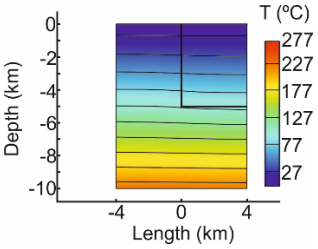

Fig. 4 2D temperature distribution simulated below Kuujjuaq

4. Discussion

Primary porosity decreases logarithmically as a function of confining pressure. These results agree with the work of Hui-yuan et al. (2016). The decrease in the primary porosity leads to an increase of thermal conductivity. For the range of confining pressure

analyzed, this increase is less than 10 %. Clauser and Huenges (1995) present a data compilation on the effect of confining pressure on thermal conductivity for granite and metamorphic rocks. These authors observed a 10 % increase on thermal conductivity within the pressure range 0 – 500 MPa.

The obtained results indicate that, for low-porosity rocks, the effect of confining pressure on thermal conductivity is minimal when compared with the influence of temperature (more than 40 %; see Miranda et al. (this volume)). Assuming only the pressure influence on thermal conductivity, at 5 km depth, a temperature of 80 °C is predicted. If only the effect of temperature is considered, then this value increases to 105 – 113 °C (Miranda et al. (this volume)). However, considering both temperature and pressure dependence on thermal conductivity, then, at 5 km depth, the temperature field simulated is 104 °C.

5. Conclusions

This work shows that 1) primary porosity decreases logarithmically as a function of confining pressure, 2) the effect of confining pressure is stronger on primary porosity than in thermal conductivity, and 3) thermal conductivity, indirectly evaluated, increases by less than 10 % as a function of the confining pressure. Considering the effect of confining pressure and temperature on thermal conductivity, a temperature of 104 °C at 5 km was simulated with a numerical heat conduction model below Kuujjuaq.

Despite the high uncertainty due to subsurface data gap, the simulated temperatures indicate potential direct use of geothermal resources to offset diesel consumption in the Canadian off-grid communities.

Acknowledgments

The authors would like to thank Felix-Antoine Comeau for the technical support during the porosity measurements. This study was funded by the *Institut Nordique du Québec* (INQ) through the *Chaire de recherche sur le potential géothermique du Nord* awarded to Jasmin Raymond. The *Centre d'études nordiques* (CEN), supported by the *Fonds de recherche du Québec – nature et technologies* (FRQNT), and the *Observatoire Homme Milieu Nunavik* (OHMI) are further acknowledged for helping with field campaigns cost and logistics.

References

Clauser, C., Huenges, E. (1995), "Thermal conductivity of rocks and minerals", in Ahrens, T.J. (editor), Rock Physics & Phase Relations: A Handbook of Physical Constants, AGU, pp. 105-126

Huy-yuan, B., Fei, W., Yong-hao, Z., Chao-wei, D., Gang, C. (2016), "Pressure-sensitivity research on porosity, permeability and acoustic slowness in tight sandstone reservoir", EJGE, 21(24), 7719-7727

Raymond J., Comeau F-A., Malo M., Blessent D., Sánchez I.J.L. (2017), "The Geothermal Open Laboratory: a free space to measure thermal and hydraulic properties of geological materials", presented at IGCP636 Annual Meeting, Santiago de Chile, 2017

Thermal conductivity from dry to water-saturated conditions: an analytical approach

Mafalda M. Miranda[1,2], Inès Kanzari[1], Jasmin Raymond[1,2]
[1.] INRS – Institut national de la recherche scientifique, Centre Eau Terre Environnement, Québec City, Canada
[2.] CEN – Centre d'études nordiques, Université Laval, Québec City, Canada
mafalda_alexandra.miranda@ete.inrs.ca

DOI: https://doi.org/10.5281/zenodo.3566001

Keywords: laboratory analyses, empirical equation, geothermal energy

Abstract

This work aims at developing a quick and reliable approach to convert thermal conductivity from dry to water-saturation conditions. The analytical approach shows a relative error between experimental and analytical values up to 10 %. This is an acceptable error to indirectly infer the thermal conductivity under water-saturation conditions.

1. Introduction

The process of water saturation of rock samples regardless of their porosity is time-consuming. It can take up to 48 h in a vacuum chamber to saturate rock samples. Moreover, the evaluation of the thermal conductivity at water-saturated conditions can easily be affected by experimental errors and not all the devices can carry out such analyses. For example, the optical scanning technique is more suited for dry rocks than for water-saturated samples. The conversion of dry bulk thermal conductivity into its respective saturated value without applying the saturation procedure can be advantageous. The goal of this work is to demonstrate an analytical approach for this conversion within a relative error up to 10 %. The approach selected is based on the mixing mean models: arithmetic, harmonic and geometric means (e.g., Fuchs et al. 2013).

2. Methods and techniques

Thermal conductivity of a set of 31 crystalline rock samples (paragneiss, diorite, gabbro, tonalite, granite) was evaluated at both dry and water-saturated conditions. The instrument used to evaluate the thermal conductivity is the FOX50 Heat Flow Meter. It analyses thermal conductivity based on the steady state method and the guarded heat flow meter technique, and as an accuracy up to 3 % (e.g., Raymond et al. 2017). Then, the effective porosity was evaluated with a combined gas permeameter-porosimeter AP-608 from Core Test following Boyle's law (e.g., Raymond et al. 2017).

Assuming rocks are represented by a two-phase system composed of pore fluid and solids, the following mixing models can be used to relate thermal conductivity and porosity:

- Arithmetic mean

$$\lambda = \phi\lambda_f + (1-\phi)\lambda_s \quad (1)$$

- Harmonic mean

$$\lambda = \frac{1}{\frac{\phi}{\lambda_f} + \frac{(1-\phi)}{\lambda_s}} \quad (2)$$

- Geometric mean

$$\lambda = \lambda_f^{\phi} \times \lambda_s^{(1-\phi)} \quad (3)$$

where λ (W m^{-1} K^{-1}) is thermal conductivity and Φ (%) is porosity. The subscripts f and s refer to the fluid-phase filling the rock voids and the solid phase, respectively.

The proposed analytical approach takes Eqs. 1 to 3 and resolves them on the basis of a system of equations for dry and saturated conditions, allowing to calculate thermal conductivity under saturated conditions:

- Arithmetic mean

$$\begin{cases} \lambda_{dry} = \phi\lambda_{air} + (1-\phi)\lambda_s \\ \lambda_{sat} = \phi\lambda_{water} + (1-\phi)\lambda_s \end{cases} \quad (4)$$

- Harmonic mean

$$\begin{cases} \lambda_{dry} = \dfrac{1}{\frac{\phi}{\lambda_{air}} + \frac{(1-\phi)}{\lambda_s}} \\ \lambda_{sat} = \dfrac{1}{\frac{\phi}{\lambda_{water}} + \frac{(1-\phi)}{\lambda_s}} \end{cases} \quad (5)$$

- Geometric mean

$$\begin{cases} \lambda_{dry} = \lambda_{air}^{\phi} \times \lambda_s^{(1-\phi)} \\ \lambda_{sat} = \lambda_{water}^{\phi} \times \lambda_s^{(1-\phi)} \end{cases} \quad (6)$$

Here, the subscripts dry and sat stand for the state at which thermal conductivity was evaluated, which are respectively, dry and water saturated. Air and water are related with the fluid filling the sample voids.

The mean relative error (MRE) was calculated to assess the inherent error of using these relationships. The *MRE* is determined as:

$$MRE = \frac{\lambda_{exp} - \lambda_{cal}}{\lambda_{exp}} \times 100 \quad (7)$$

where the subscripts exp and cal stand for the thermal conductivity evaluated and calculated, respectively.

3. Results

The results reveal an increase in thermal conductivity from dry to water-saturated state in most of the lithological groups (**Table 1**). On average, the thermal conductivity increases by 18 % for the paragneiss, 11 % for the diorite, 10 % for the gabbro, 15 % for the tonalite, and decreases by 2 % for the granite. This decrease is thought to be due to the intrinsic accuracy of the device rather than the experimental procedure itself.

Table 1 Group averaged values for each thermophysical parameter

Lithology	λ_{dry}	λ_{sat}	Φ
	(W m^{-1} K^{-1})		(%)
Paragneiss	2.26	2.67	2.81
Diorite	2.78	3.08	2.05
Gabbro	2.93	3.21	2.05
Tonalite	3.02	3.47	2.29
Granite	3.22	3.17	2.85

A comparison of thermal conductivity with the effective porosity reveals that samples with a low effective porosity show a smaller increase in thermal conductivity associated to saturation than more porous samples.

Applying arithmetic and harmonic mean models (Eq. 4, 5) to convert thermal conductivity from dry to water-saturated conditions leads to a relative error of more than 20 %. Smaller relative error is obtained by applying the geometric mean model (Eq. 6; **Table 2**).

Table 2 Thermal conductivity at water-saturation conditions, experimental *vs* analytical methods

Lithology	λ_{exp}	λ_{cal}	*MRE*
	(W m^{-1} K^{-1})		(%)
Paragneiss	2.67	2.46	8
Diorite	3.08	2.96	4
Gabbro	3.21	3.12	3
Tonalite	3.47	3.23	7
Granite	3.17	3.51	-11

The use of this analytical approach, for this dataset, leads to a relative error up to 10 %. This analysis points that this simple analytical approach can be a helpful tool to convert thermal conductivity from dry to water-saturated conditions.

4. Discussion

Fuchs et al. (2013) did a similar study with sedimentary rocks and concluded that the geometric mean model displays the best correspondence between measured and calculated thermal conductivity. However, these authors indicated that the relation was not fully satisfactory. Their approach relied on correction equations calculated based on the statistical data to improve the fit of the models. For this study, the relationship is satisfying. However, further work is needed to verify if the relative error stays low when applying the same approach to other rock types.

Additionally, this analytical approach can also be used to evaluate the effect of temperature on thermal conductivity of water-saturated samples. Carrying out such analysis at different temperature ranges is only possible for samples at dry state, due to water evaporation. However, with this analytical approach, saturated thermal conductivity can be calculated from dry thermal conductivity evaluated at high temperature.

5. Conclusions

A quick and reliable approach to convert thermal conductivity from dry state to water-saturation conditions was described in this work. The thermal conductivity inferred indirectly by this analytical approach has a relative error up to 10 % when compared with the experimental procedure.

Acknowledgments

This study was funded by the *Institut Nordique du Québec* (INQ) through the *Chaire de recherche sur le potential géothermique du Nord* awarded to Jasmin Raymond.

References

Fuchs S., Schütz F., Förster A., Förster H-J. (2013), "From dry to saturated thermal conductivity: mixing-model correction charts and new conversion equations for sedimentary rocks", presented at General Assembly European Geosciences Union, Vienna, 2013 April 7 - 12

Raymond J., Comeau F-A., Malo M., Blessent D., Sánchez IJL. (2017), "The Geothermal Open Laboratory: a free space to measure thermal and hydraulic properties of geological materials", presented at IGCP636 Annual Meeting, Santiago de Chile, 2017 Nov 21

Fluid origin and dynamic at the newly developed Theistareykir geothermal field, Iceland

Marion Saby[1*], Daniele L. Pinti[1], Vincent van Hinsbger[2], Bjarni Gautason[3], Ásgerður K. Sigurðardóttir[4], Clara Castro[5], Chris Hall[5], Jean-François Hélie[1], Océane Rocher[1]

[1.]GEOTOP & Département des sciences de la Terre et de l'atmosphère, Université du Québec à Montréal, 201 Av. du Président Kennedy, Montréal, Canada
[2.] GEOTOP & Department of Earth and Planetary sciences, McGill University, 34, University Street, Montréal, Canada
[3.] ÍSOR Iceland GeoSurvey, Orkugardur, Grensásvegur 9, Reykjavik, Iceland
[4.] Landsvirkjun, Háaleitisbraut 68, Reykjavik, Iceland
[5.] Department of Earth and environmental sciences, University of Michigan, Ann Arbor, USA
marion.saby23@gmail.com

DOI: https://doi.org/10.5281/zenodo.3566003

Keywords: Noble gas isotopes, Water isotopes, Geothermal field, Theistareykir, Iceland

Abstract

This study aim at deciphering the origin of the fluids and the hydrodynamic of the Theistareykir geothermal system using water isotopes and noble gases as a tracer of these respective contributions. Results first confirm that the magma beneath Theistareykir is a mix between a mantle plume (OIB) and an ocean ridge basalt (MORB). They also show that both magmatic fluids and surface water are present in the system in proportions that are being quantifyed. Water isotopes show that sources of surface water range from modern to Pre-Holocene. A crustal input is also present in the system with an enrichment in $\delta^{18}O$ highlighting water-rock interaction.

1. Introduction

Here we discuss results from Theistareykir, a high-enthalpy geothermal field developed in the Northern Volcanic Zone (NVZ) of Iceland, set on the mid-Atlantic oceanic ridge (Óskarsson et al 2015). Noble gases and water isotopes have been chosen as a privileged geochemical and isotopic tool to determine the sources of fluids in the system and monitor the system dynamic (Pinti et al., 2017). They can help the contributions of purely magmatic fluids versus fluids impacted by leaching of host rocks (crustal fluids) using the helium isotopic ratio $^{3}He/^{4}He$ or the argon isotopic ratio $^{40}Ar/^{36}Ar$. Noble gases elemental ratios are also very helpful to constrain solubility-driven processes such as boiling, steam condensation which are crucial processes in understanding magmatic and hydrothermal systems' dynamic (Burnard 2001, Fisher 1997, Hedenquist and Lowenstern,1994).

2. Methods and techniques

Water isotopes were analyzed at GEOTOP by Isotope Ratio Infrared Spectrometer with two lasers for the simultaneous measurements of δ18O and δ2H by Off-Axis Integrated Cavity Output Spectroscopy. Helium isotopes were analyzed at GEOTOP at the University of Québec in Montréal (UQAM) by a Pfeiffer® PRISMA-200 quadrupole mass spectrometer and Thermo® HELIX MC Plus multi-collection mass spectrometer, and at the Noble Gas Laboratory at the University of Michigan (Ma et al 2005, Castro et al 2009).

3. Results

Water isotopes show a wide range of values, especially with $\delta^{2}H$ with values ranging from -100.08 ‰ to -119.29 ‰ and $\delta^{18}O$ ranging from -19.61 ‰ to -8.50 ‰ mud pots, fumaroles and wells together. Rc/Ra ratio range from 3.00 to 11.45 showing both atmospheric, MORB and hot spot influences on the system. The crustal component seems to have less influence. Noble gas elemental ratios $^{132}Xe/^{36}Ar$ and $^{84}Kr/^{36}Ar$ show values ranging from 0.977 to 4.612 and from 0.976 to 1.878 respectively.

4. Discussion

The first results from noble gases (**Fig. 1**) confirms that the magma beneath Theistareykir is a mix between approximately 87,5 % of the mantle beneath the oceanic ridge and 12.5 % of the Icelandic hotspot. The mean $^{3}He/^{4}He$ ratio is 11Ra, when a typical MORB is 8±1Ra.

Fig. 2 shows that the field is recharged by Pre-Holocene meteoric water (Sveinbjornsdottir et al., 2013) as suggested by very depleted $\delta^{2}H$ values and the presence of radiogenic $^{40}Ar^{*}$.

Relation between the heat flow and the ^{3}He excesses ($Q/^{3}he$) indicate that the northeastern zone of the field is directly influenced by magma degassing. The elemental ratios $^{132}Xe/^{36}Ar$ and $^{84}Kr/^{36}Ar$ indicate that the reservoir is not yet affected by boiling or re-injection effects. Hot fluids have deeply altered the reservoir, as

indicated by the $\delta^{18}O$ shift and a slight increase in radiogenic ^{4}He and $^{40}Ar^{*}$ derived from local reservoir rocks.

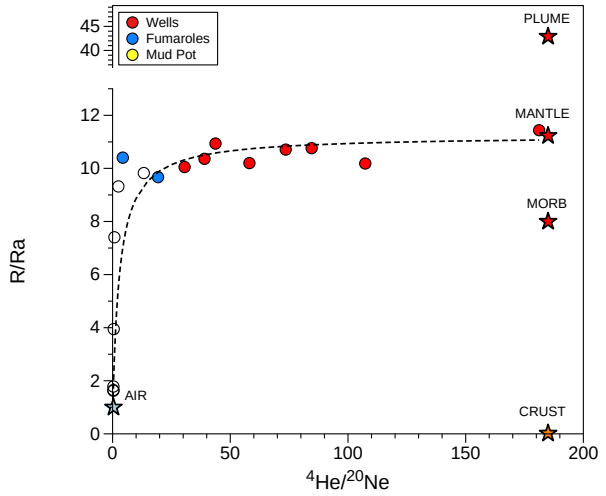

Fig. 1 Isotopic values of helium (Rc/Ra ratio) against the 4He/20Ne isotopic ratio showing the dominant mantle source of helium.

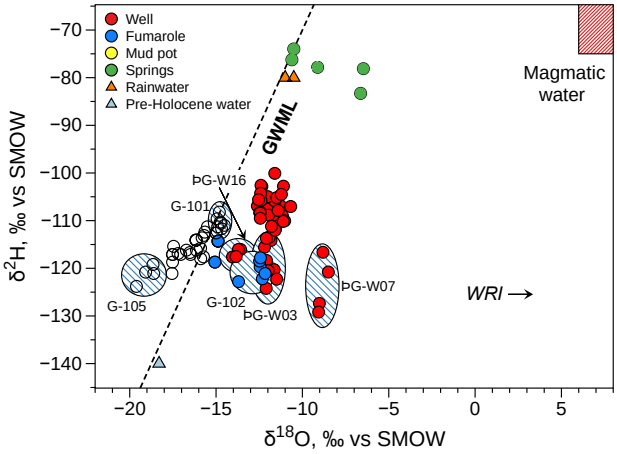

Fig. 2 Water isotopic composition of $\delta^{18}O$ and $\delta^{2}H$ from the water discharge of the wells and from the surface mud pots and fumaroles compare to surface springs and the hypothetical Pre-Holocene water component.

5. Conclusions

The two main sources of magma have been confirmed in Theistareykir using helium and neon isotopes. Water isotopes showed the presence of multiple fluids in the geothermal system and both noble gases and water isotopes helped understand the dynamic of the system by highlighting processes such as water-rock interaction and magma degassing.

Acknowledgments

The authors would like to thanks the Natural Sciences and Engineering Research Council of Canada (NSERC) for the financial support.

References

Burnard, P., 2001. Correction for volatile fractionation in ascending magmas: noble gas abundances in primary mantle melts. Geochimica et Cosmochimica Acta, 65(15): 2605-2614.

Castro, M.C., Ma, L., Hall, C.M., 2009. A primordial, solar He-Ne signature in crustal fluids of a stable continental region. Earth Planet. Sci. Lett. 279, 174-184.

Fischer, T.P., Sturchio, N.C., Stix, J., Arehart, G.B., Counce, D. and Williams, S.N., 1997. The chemical and isotopic composition of fumarolic gases and spring discharges from Galeras Volcano, Colombia. Journal of Volcanology and Geothermal Research, 77(1): 229-253.

Hedenquist, J.W. and Lowenstern, J.B., 1994. The role of magmas in the formation of hydrothermal ore deposits. Nature, 370(6490): 519-527.

Ma, L., Castro, M.C., Hall, C.M., Lohmann, W.M., 2005. Cross-formational flow and salinity sources inferred from a combined study of helium concentrations, isotopic ratios and major elements in the Marshall aquifer, southern Michigan. Geochem. Geophys. Geosyst. 6, Q10004. http://dx.doi.org/10.1029/2005GC001010.

Óskarsson, F., Ármannsson, H., Ólafsson, M., Sveinbjörnsdóttir, Á.E. and Markússon, S.H., 2015. The Theistareykir Geothermal Field, NE Iceland: Fluid Chemistry and Production Properties. Procedia Earth and Planetary Science, 7: 644-647.

Pinti, D.L., Castro, M.C., Lopez-Hernandez, A., Han, G., Shouakar-Stash, O., Hall, C.M. and Ramírez-Montes, M., 2017. Fluid circulation and reservoir conditions of the Los Humeros Geothermal Field (LHGF), Mexico, as revealed by a noble gas survey. Journal of Volcanology and Geothermal Research, 333: 104-115.

Sveinbjornsdottir, Á., Ármannsson, H., Ólafsson, M., Óskarsson, F., Markússon, S. and Magnusdottir, S., 2013. The Theistareykir geothermal field, NE Iceland. Isotopic characteristics and origin of circulating fluids. Procedia Earth and Planetary Science, 7: 822-825.

Poroelasticity of hydraulic fracturing of a reservoir

Miad Jarrahi[1], Hartmut Holländer[2]

[1.]Ph.D. candidate, Department of Civil Engineering, University of Manitoba, Winnipeg, Canada
[2.]Associate professor, Department of Civil Engineering, University of Manitoba, Winnipeg, Canada
jarrahim@myumanitoba.ca

DOI: https://doi.org/10.5281/zenodo.3566007

Keywords: hydraulic fracturing, fractured reservoir, discrete rough natural fractures, poroelasticity

Abstract

The development of numerical simulation of unconventional shale gas reservoirs has been accelerated due to its major contribution in hydrocarbon production. In this study, the developed mode hydro-fractures interact with pre-existing natural fractures and create a fracture network, which later create a fluid flow network, within the reservoir rock. The objective of this study is to simulate the poroelastic response of the rock formation during the extension of fluid flow within the fractures network. It was investigated that the far field poroelastic behavior of the reservoir triggers the rock whether to show elastic or plastic deformation, while the effect of stresses induced fracture propagation is neglected.

1. Introduction

Hydraulic fracturing (or fracking) is the hydraulic stimulation by injecting pressured water into a borehole to increase permeability of the formation. The formation with enhanced permeability is more efficient for hydrocarbon exploitations. During the hydraulic stimulation, tensile stress within the rock matrix may exceed its tensile strength and cause tensile fracture. The resulting tensile fractures (i.e. hydro-fractures) may join to each other and to existing natural fractures and create a network of interconnected fractures. The pore pressure is a key factor in tensile rock fracture. The direction and the extension of fluid flow within the fracture network depend on pore pressure distribution, specifically (Bruno, Dorfmann et al.). The complexity of hydraulic fracturing was addressed by Adachi, Siebrits et al. (2007). In their study, the hydraulic fracturing was noted as a complicated process, which involves three other coupled processes: (i) the rock deformation induced by the pore pressure; (ii) the flow of fluid within the fracture; and (iii) the fracture's mechanical response. Either mechanical response of rock or fracture was modeled using the theory of linear elastic mechanics. The linear elastic fracture mechanics (LEFM) theory provides the conventional energy-release rate approach to define the criterion for fracture propagation. In this literature review, it is noticed that among the numerical studies, the discrete fracture network was not simulated while it is coupled to the single continuum rock matrix. Therefore, a thorough investigation of poroelastic behavior of the rock formation in response to the fluid flow and its extension within the fracture network was not performed. The deformation of reservoir rock due to the newly developed hydro-fractures was studied by Jacquey, Cacace et al. (2017). The impact of fracture growth on the rock hydraulic properties was addressed in their work, however, no natural fracture was considered. They showed that the diffusive processes and poroelastic effects are responsible for sudden local increase in pore pressure within the matrix. Their results indicated the importance of poroelastic behavior of stimulated reservoir rock.

In this study, the stimulated reservoir volume (SRV) modeling technique is integrated with the finite element approach to simulate a 3-D poroelastic porous matrix coupled with a discrete fracture network. The major objective of this paper is to numerically investigate the rock formation deformation induced fluid flow within the discrete fracture network during the hydraulic fracturing under following assumptions. The SRV is considered to be a typical 100×100×100 m homogeneous shale rock formation with a centered horizontal wellbore, parallel horizontal plate-like natural fractures, and vertical circular hydro-fractures. The stress field induced fractures growth is neglected due to the enhancement of large scale modeling. Therefore, the hydro-fractures aperture and radius are assumed to remain constant during the transient numerical simulations. However, to investigate the effect of fracture growth on the extension of fluid flow network, different hydro-fractures radius was considered for different models. Each model accounts as an increment of hydraulic fracturing operation.

2. Model Description

The poroelastic response due to the fluid flow extension within a network of hydro-fracture and natural fractures was studied in Barnett Shale, central-eastern Texas, US. The Barnett Shale is the most mature of the currently producing gas shale plays in US (Fan, Luo et al. 2011). This Paleozoic reservoir, located in the Bend

Arch Fort Worth Basin area, is a middle- to late-Mississippian organic-rich shale and discovered to be productive since the early 2000's including (Montgomery, Jarvie et al. 2005, Sone 2012). The thickness of the Barnett Shale varies from 15-30 m in the southwest, up to 300 m in the northeast at the Newark East Field area, (Montgomery, Jarvie et al. 2005). The variation of the viscoelastic properties of Barnett Shale was reported by Sone (2012). The in-situ stress field of the reservoir was stated using the Formation Micro-Imager (FMITM) from a vertical wellbore. The viscoelastic parameters and in-situ stresses of the formation at the depth of ~2600 m are summarized in Table 1. Natural fractures were mostly observed at the depth of 2600-2660 m, where the basal hot shale section is located. The strike and dip of the fractures were reported as N50W, 80-85°, respectively (Sone 2012).

Table 1 The viscoelastic parameters and in-situ stresses.

Parameter	Value at depth of ~2600 m
Vertical in-situ stress	65 MPa
Minimum horizontal in-situ stress	47 MPa
Maximum horizontal in-situ stress	85 MPa
Pore pressure	30.5 MPa

In the current study, a horizontal wellbore, was considered within the basal hot shale section of the formation, where the axis of the wellbore is aligned with a horizontal in-situ stress. Either orientation I (*i.e.* perpendicular to wellbore axis) or orientation II (*i.e.* parallel to wellbore axis) of the hydraulic fracture may occur, depending on the direction of the wellbore. Therefore, orientation I occurs when the wellbore axis is parallel to the maximum horizontal in-situ stress (i.e. N20E). Orientation II occurs when the wellbore is perpendicular to the maximum horizontal in-situ stress (*i.e.* N110E).

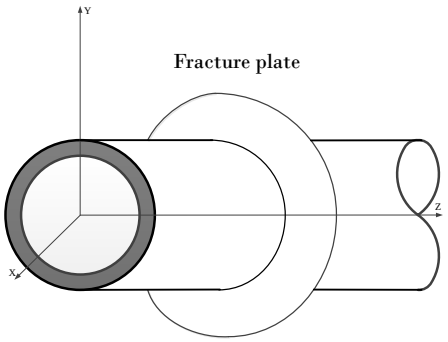

Fig. 1 Hydro-fracture orientation I at depth of 2600-2660 m.

3. Results

The preliminary contours of pressure and hydraulic head at the last propagation increment, shown in Fig. 2 and 3, illustrated that the existing natural fractures triggered a path of least resistance to the static pressure that is imposed by intersected hydro fractures. Therefore, new highly permeable regions were accessible to the fluid flow throughout the reservoir.

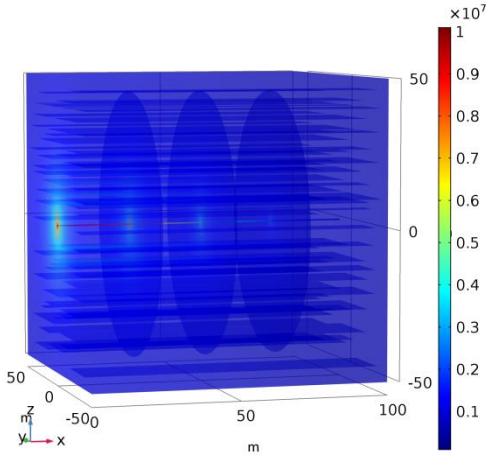

Fig. 2 Contour of pressure at the last propagation increment.

The fluid flow formed in both vertical plates of hydro fractures as well as horizontal plates of natural fractures. The horizontal flow showed reverse directions at each stage of perforation, thus, created the pressure reinforcement at the vicinity of each hydro fracture.

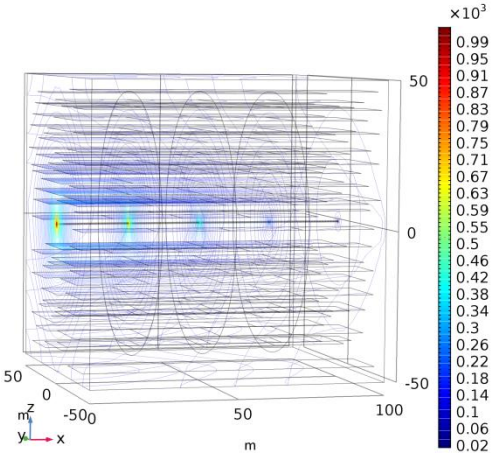

Fig. 3 Contour of hydraulic head at the last propagation increment.

4. Conclusions

This numerical study was conducted to address the propagation of the hydro fractures in two different orientations. The results of these simulations are presented as one quasi-transient simulation as fracture propagates. The advantage of this method is the

dramatic reduction in computational effort and efficient approach to investigate the growth of fractures. In addition, the system of the natural fracture network (SNFN) was generated in horizontal plates based on laminated and fissile feature of shale gas reservoirs, evidenced in shale outcrops. In the results, the impact of the current realisation of SNFN on the stimulated reservoir volume was evaluated during the interaction of hydro fractures with natural fractures. It was also seen that the natural fractures opening became wider during the hydraulic fracturing. The consequences of opening the horizontal plate-like natural fractures during the hydraulic fracturing were investigated due to poroelastic behaviour of porous matrix. Lastly, a substantial permeability was then created due to the fact that the network of the horizontal plate-like natural fractures became connected via vertical hydro fractures.

References

Adachi, J., E. Siebrits, A. Peirce and J. Desroches (2007). "Computer simulation of hydraulic fractures." International Journal of Rock Mechanics and Mining Sciences 44(5): 739-757.

Bruno, M. S., A. Dorfmann, K. Lao and C. Honeger Coupled particle and fluid flow modeling of fracture and slurry injection in weakly consolidated granular media. in Rock Mechanics in the National Interest: Proceedings of the 38th U.S. Rock Mechanics Symposium.

Fan, L., F. Luo, G. J. Lindsay, J. W. Thompson and J. R. Robinson (2011). The Bottom-Line of Horizontal Well Production Decline in the Barnett Shale. SPE Production and Operations Symposium. Oklahoma City, Oklahoma, USA, Society of Petroleum Engineers: 10.

Jacquey, A. B., M. Cacace and G. Blöcher (2017). "Modelling coupled fluid flow and heat transfer in fractured reservoirs: description of a 3D benchmark numerical case." Energy Procedia 125: 612-621.

Montgomery, S., D. Jarvie, K. Bowker and R. Pollastro (2005). "Mississippian Barnett Shale, Fort Worth basin, north-central Texas: Gas-shale play with multi–trillion cubic foot potential." AAPG Bulletin 89: 155-175.

Sone, H. (2012). Mechanical properties of shale gas reservoir rocks and its relation to the in-situ stress variation observed in shale gas reservoirs. Ph.D. thesis, Stanford University.

Assessment of groundwater contribution to surface water quantity, quality and temperature in rivers of northern Quebec

Milad Fakhari[1], Jasmin Raymond[2], Richard Martel[2]

[1.] PhD in Earth sciences (INSTITUT NATIONAL DE LA RECHERCHE SCIENTIFIQUE, Centre Eau-Terre-Environnement, Québec, Québec)
[2.] Professor (INSTITUT NATIONAL DE LA RECHERCHE SCIENTIFIQUE, Centre Eau-Terre-Environnement, Québec, Québec)
milad.fakhari@ete.inrs.ca

DOI: https://doi.org/10.5281/zenodo.3566009

Keywords: surface water-groundwater interaction, permafrost, heat transport, climate change

Abstract

Surface water-groundwater (SW-GW) interaction has an important role on quantity and quality of water resources as well as health of aquatic systems. Since the temperature of groundwater and rivers are different, the movement of water means transport of heat. Due to presence of permafrost and freeze-thaw cycle of active layer in northern Quebec, the physics controlling SW-GW interaction varies from one pint to another as well as from one season to another. SW-GW interaction in these regions is highly controlled by temperature dependent parameters. Climate change can have noticeable effect on future of SW-GW interaction and aquatic systems in these regions.

1. Introduction

The research questions that are going to be addressed are:
I) At what locations the groundwater-surface water interaction is present?
II) What parameters control this interaction?
III) To what extent the rivers' thermal budget can be affected by groundwater?
IV) Can permafrost help reduce contaminant transport to the rivers?
To see the effect of permafrost and climate on movement of water, contamination and heat from groundwater to rivers, two sites on two different rivers located on different climates and permafrost condition have been selected for detailed studies.

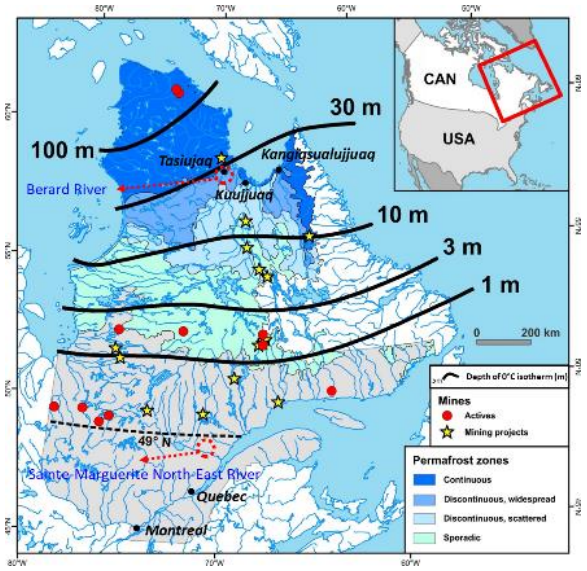

Fig. 1 Location of two selected rivers on permafrost map of Quebec.

2. Methods and techniques

The methodology can be summarized into two main parts: field measurements and modelling. Field measurements are required since there are no hydrological data available for the selected sites. Moreover, the detailed continuous data will be used for model calibration and history matching in order to have a more reliable prediction from the models. Modelling will be done using COMSOL software. The model will combine free flow (flow in the river), groundwater flow (saturated and unsaturated flow) and heat transport to simulate water and heat circulation in the system.

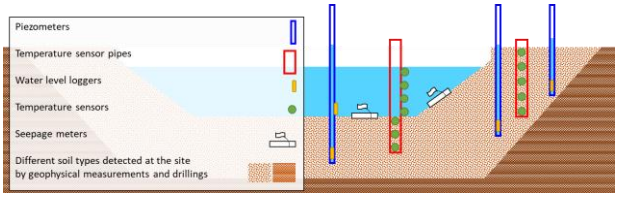

Fig. 2 Summary of all field measurements on the study site in cross-section view.

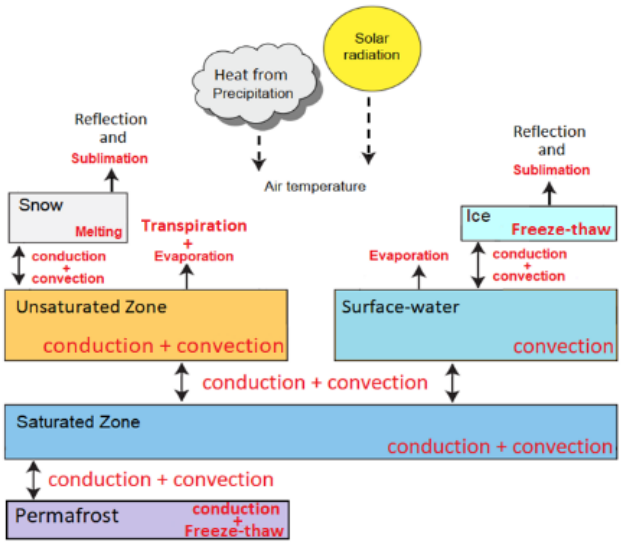

Fig. 3 Schematization of water circulation (black arrows) and methods of heat transport (in red) in the system.

3. Discussion

Change in the flow pattern modulates the temperature distribution in the system; since heat transport due to convection is significant in surface water-groundwater interaction modelling.

Even a small section of permafrost (sporadic) can significantly change the groundwater flow system. The freeze-thaw cycle of permafrost and active layer (layer on top of permafrost) causes the quantity of surface water-groundwater interaction to vary in summer and winter. Therefore, considering all terms of conduction, convection and phase change as methods of energy transport is important.

Geothermal energy potential in southwestern New Brunswick

Nadia Mohammadi[1,2]

[1]Carleton University, Department of Earth Sciences, Ottawa, ON, Canada
[2]University of New Brunswick, Department of Earth Sciences, Fredericton, NB, Canada
nadia.mohammadi@unb.ca

DOI: https://doi.org/10.5281/zenodo.3566011

Keywords: High Heat Production Mount Douglas Granite, Radiogenic Heat Production, Geothermal Energy, Southwestern New Brunswick, Uraniferous Granite

Abstract

The high heat production (HHP) Mount Douglas Granite has elevated concentrations of K_2O, Rb, LREE, U, and Th in response to high degrees of fractional crystallization. The uraniferous granite produces anomalous heat generated by radiogenic decay of unstable isotopes, such as ^{238}U, ^{232}Th, and ^{40}K. The average weighted mean radiogenic heat production of the granite assuming a density of 2.61 g/cm^3 is 5.9 μW/m^3 (14.1 HGU) which is significantly higher than the average of upper continental crust (1.65 μW/m^3). The high HGU of the granite supports its assignment to a 'hot crust' (>7 HGU) HHP granite and highlights its potential for a local, renewable, sustainable, and clean geothermal energy exploration.

1. Introduction

The Late Devonian Mount Douglas Granite (368 ± 3 Ma (Mohammadi, 2018), located in Southwestern New Brunswick, ~40 km east of the Mount Pleasant W–Mo–Bi and Sn–Zn–Cu–In deposits, forms the eastern part of the Late Silurian to Late Devonian Saint George Batholith (Fig. 1). The intrusion is composed of a suite of metaluminous to peraluminous leucogranitic rocks that apparently evolved from a zoned magma chamber in a three-stage process, resulting in compositionally and chronologically distinct units (Fig. 1), i.e., units Dmd1, Dmd2, and Dmd3 (McLeod, 1990). The radiogenic heat production of the Mount Douglas Granite was examined in this study to determine any potential of Hot Dry Rock (HDR) geothermal resources in this area.

2. Methodology and Results

The radiogenic heat production rates of the units Dmd1, Dmd2, and Dmd3 were calculated using whole-rock geochemical data taken from Mohammadi (2018; laser ablation ICP-MS analyses on fused glass beads produced *in house*) and McLeod (1990) following an equation developed by Rybach (1988):

$$A\ [\mu W/m^3] = 10^{-5} \times \rho\ [kg/m^3] \times (2.56 \times C_{Th}\ [ppm] + 9.52 \times C_U\ [ppm] + 3.48 \times C_K\ [\%])$$

where A is heat production and ρ is density (2.61 g/cm^3). The C_U and C_{Th} are the concentrations of U and Th (in ppm), respectively, and C_K is the concentration of K in wt.%. The estimated weighted mean radiogenic heat production of the granite is 4.67, 5.65, and 6.93 (μW/m^3) for Dmd1, Dmd2, and Dmd3, respectively (Table 1).

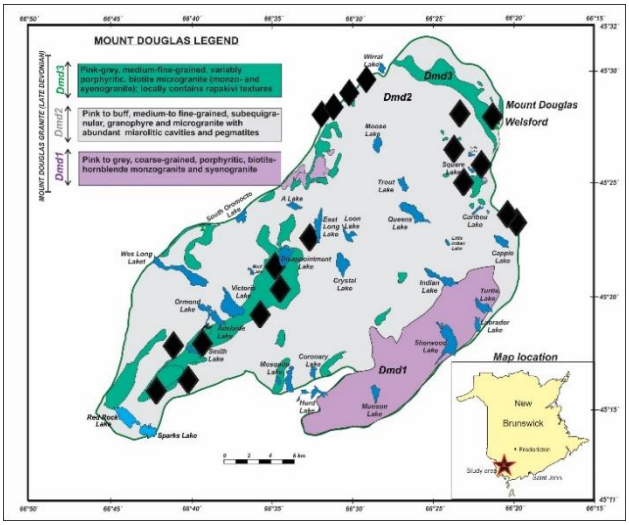

Fig. 1 Geology of the Mount Douglas Granite with units Dmd1, Dmd2, and Dmd3 (modified after McLeod 1990; Mohammadi et al. 2017). Black diamonds are mineral occurrences associated with the Mount Douglas Granite, and compiled from the Metallogenic Map of New Brunswick, NR-7 (2002). The mineral occurrences consist of Sn, W, Mo, Zn, and Bi-bearing greisen and sheeted veins.

Table 1 Weighted mean Th (ppm), U (ppm), and K_2O (wt.%) contents for units Dmd1, Dmd2, and Dmd3 of the Mount Douglas Granite and their radiogenic heat production rates, A (μW/m^3).

Unit	Density	Th	U	K_2O	A
Dmd1	2610	38.0	6.7	5.2	4.59
Dmd2	2610	40.2	10.1	5.0	5.58
Dmd3	2610	50.1	12.6	4.9	6.85
Upper Continental Crust	-	10.5	2.7	-	1.65

Note: Data for units Dmd1, Dm2, and Dmd3 are from Mohammadi, McFarlane, and Lentz (2019). The average upper continental crust values are from Rudnick and Gao (2003).

3. Discussion

The high radiogenic heat production of the Mount Douglas Granite, accompanied by a high estimated heat flow of 70 mW/m^2 (Chandra, 1980) is comparable to other locations that have been classified as HHP granites (e.g., Leat et al. 2018; Sun et al. 2015) support the assignment of the granite to a 'hot crust' (>7 HGU) HHP granite and highlights its potential for geothermal energy exploration. This could be a local, renewable and clean energy source associated with deep hot crystalline rocks with temperatures generally higher than 150°C. Such high heat production is expected to result in local heat flow anomalies for the area, although further investigation, such as airborne radiometric surveys, seismic data, and satellite magnetic data, are required.

4. Conclusions

Results obtained from this study demonstrate that the Mount Douglas granitic rocks may have great potential for dry geothermal energy sources; however, surface heat flow, which is a function of radioactive element contents below the continents, the latest thermal event, and the intensity of tectonic activities are important parameters that should be considered when evaluating potential geothermal resources.

Acknowledgments

The author is grateful to Dr. Dave Lentz and Dr. Chris McFarlane (Department of Earth Sciences, University of New Brunswick, UNB). This work was supported by New Brunswick Energy and Resource Development, President's Doctoral scholarship (UNB), New Brunswick Innovation Foundation (NBIF), and W.J. Wright Graduate Fellowship (UNB).

References

Chandra, J. J. (1980). New Brunswick Radioactive Heat Product. *New Brunswick Department of Natural Resources Branch, Plate 80-92*.

Leat, P. T., Jordan, T. A., Flowerdew, M. J., Riley, T. R., Ferraccioli, F., & Whitehouse, M. J. (2018). Jurassic high heat production granites associated with the Weddell Sea rift system, Antarctica. *Tectonophysics*, *722*(12), 249–264. https://doi.org/10.1016/j.tecto.2017.11.011

McLeod, M. J. (1990). *Geology, Geochemistry and Related Mineral Deposits of the Saint George Batholith; Charlotte, Queens and Kings Counties, New Brunswick*. New Brunswick, Natural Resources and Energy, Mineral Resources Report 5, 169 p.

Mohammadi, N. (2018). *Petrogenesis of tin-tungsten-molybdenum mineralized intragranitic systems within the highly evolved Mount Douglas polyphase intrusive complex, southwestern New Brunswick, Canada. Unpublished PhD Dissertation*. University of New Brunswick.

Mohammadi, N., Fyffe, L., McFarlane, C. R. M., Thorne, K. G., Lentz, D. R., Charnley, B., and Butler, S. (2017). Geological relationships and laser ablation ICP-MS U-Pb geochronology of the Saint George Batholith, southwestern New Brunswick, Canada: implications for its tectonomagmatic evolution. *Atlantic Geology*, *53*, 207–240. https://doi.org/10.4138/atlgeol.2017.008

Mohammadi, N., McFarlane, C. R. M., & Lentz, D. R. (2019). U–Pb geochronology of hydrothermal monazite from uraniferous greisen veins associated with the high heat production Mount Douglas Granite, New Brunswick, Canada. *Geosciences*, *9*(5), 224. https://doi.org/10.3390/geosciences9050224

Rudnick, R. L., & Gao, S. (2003). Composition of the continental crust. *Treatise on Geochemistry*, *3*, 1–64.

Rybach, L. (1988). Determination of heat production rate. In R. Hänel, L. Rybach, & L. Stegena (Eds.), *Handbook of Terrestrial Heat Flow Density Determination* (pp. 125–142). Kluwer, Dordrecht.

Sun, Z., Wang, A., Liu, J., Hu, B., & Chen, G. (2015). Radiogenic heat production of granites and potential for hot dry rock geothermal resource in Guangdong Province, Southern China. *World Geothermal Congress 2015*, (April), 2–6.

Numerical simulations of oscillatory thermal response tests

Nicolò Giordano[1], Vincent Chapotard[2], Louis Lamarche[2], Jasmin Raymond[1]

[1.] Institut national de la recherche scientifique (INRS), Centre Eau Terre Environnement, Québec City, Canada
[2.] École de technologie supérieure (ÉTS), Montréal, Canada
nicolo.giordano@ete.inrs.ca

DOI: https://doi.org/10.5281/zenodo.3566014

Keywords: oscillatory thermal response test, thermal conductivity, heat capacity, numerical simulation

Abstract

Thermal response tests are the most popular in-situ technique to assess ground thermal conductivity and borehole thermal resistance. Conventional tests with a constant heat injection rate do not allow to infer the ground heat capacity. Oscillatory tests are proposed as a tool to evaluate subsurface thermal diffusivity and estimate the heat capacity. Numerical simulation results showed that the frequency of heat injection and the radius of the U-pipe have a significant influence on the temperature response of such tests. The grout's thermal properties and the borehole heat storage effect are main issues to face in order to evaluate the ground heat capacity. Oscillation periods longer than 12 h can however help to have proper penetration depth and limit the borehole influence.

1. Introduction

Thermal response test (TRT) is the most common field method to estimate the subsurface thermal conductivity and the borehole thermal resistance for ground source heat pump systems. Hot water is circulated within the borehole heat exchanger (BHE) in order to inject 50 to 80 W/m (Kavanaugh 2001; Spitler and Gehlin 2015) during conventional TRTs. Low-power tests (10-25 W/m) can also be conducted with heating cables and demonstrated to provide accurate results (Raymond et al. 2015). Tests are commonly carried out for 48 to 72 h with a constant power. TRTs with step heat injection have also been proposed to determine optimal heat rejection/extraction rates (Kurevija et al. 2018).

This study describes the use of an oscillatory heat source in replacement of a common constant power. The hypothesis is that the thermal response of an oscillatory thermal response test (O-TRT) will be affected by heat storage and will provide more information about subsurface and borehole thermal properties when compared to conventional TRT (Oberdorfer 2014). Oscillatory pumping tests have been proposed in hydrogeology as a practical and effective technique for establishing local-scale spatial variability in hydraulic parameters (Guiltinan and Becker 2015). The phase shift and the amplitude attenuation of the recorded signal are functions of the transmissivity and storativity of the aquifer. Analogously, the thermal conductivity (TC) and heat capacity (HC) of the subsurface can be estimated by the analysis of a similar test in the heat transport domain.

The present contribution aims at defining the most influencing parameters of O-TRT through a parametric numerical study as a preparatory step before moving to field testing. An optimal heat injection protocol is therefore outlined for conducting experiments with both water circulation and heating cable.

2. Methods and techniques

The numerical simulations were carried out with COMSOL Multiphysics® (COMSOL 2019). A 2-D circular model with diameter of 40 m was built to simulate a single-U pipe borehole heat exchanger (diameter 152 mm). A parametric analysis was conducted to evaluate the influence of 11 parameters on the results, namely the thermal properties of the grout, subsurface and heat carrier fluid; the period, amplitude and duration of the oscillations; the diameter of the borehole and the pipes, and the shank spacing. The time steps were set to 0.1 h and, after a mesh independency analysis, the number of triangular elements was set to 9806, the maximum and minimum size of the elements being 0.3 and 0.008 m.

3. Results and Discussion

The frequency of the oscillation is a crucial parameter defining the target of the test, and has the highest influence of the phase shift between the source (heat injection) and the recorded signal (temperature). The results show that the oscillation frequency has the highest average deviation (13.3 %) from the base-case value among all the parameters considered. The minimum, base-case and maximum periods considered are 0.67, 4 and 30 h, respectively. The radius of the U-pipe follows with 11.1 %. Thermal conductivity (2.5 %) and heat capacity (0.8 %) of the backfilling material have a larger influence than the equivalent subsurface properties with 0.17 % and 0.2 %. In particular, doubling the grout HC will result in a larger signal difference on the phase shift than doubling the subsurface HC (**Fig. 1**). Therefore, as expected, the heat

storage effect of the BHE is the largest obstacle to the evaluation of the subsurface HC, but a longer oscillation period result in a smaller BHE influence. A similar study by Oberdorfer (2014) show that high-frequency tests have small penetration depths and can highlight anomalous borehole thermal resistance due to flaws of the geothermal grouting. On the other hand, high-period tests (low frequencies) are necessary to increase the penetration depth to more than 10 cm and significantly affect the subsurface.

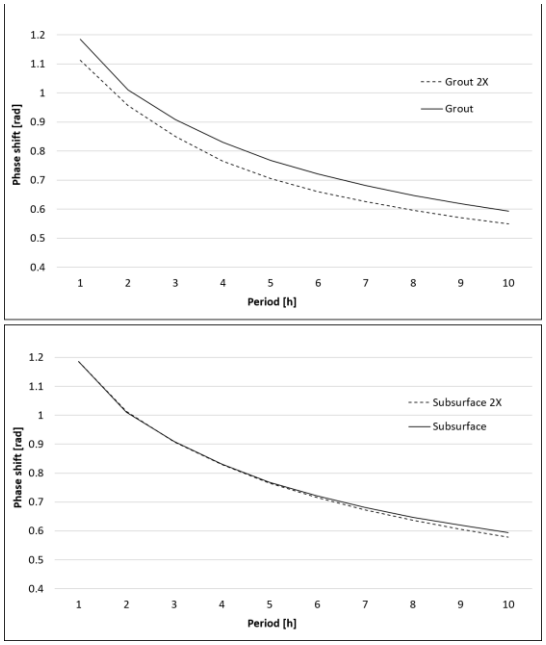

Fig. 1 Comparison between the phase shift of the temperature signal when doubling the heat capacity of the BHE grout (upper graph) and the subsurface (lower graph).

4. Conclusions

A heat injection protocol with period of 12 h, offset of 35 W/m, amplitude of 15 W/m and duration of 48 h has been chosen to move towards field testing with water circulation. Heating cables O-TRT will have smaller offset (20 W/m) and amplitude (5 W/m); both parameters demonstrated to have no influence on the results. Based on this preliminary study and on the response time of the temperature sensors available for field work (20-seconds accuracy, Fig. 2), the subsurface heat capacity can be estimated with a resolution of 0.5 MJ/m^{3}K, i.e. the 19 % of a base-case 2.6 MJ/m^{3}K. Resolution can be increased with longer periods (15 % at 24 h) or more accurate sensors (16 % with 10-seconds accuracy). The linear component of the temperature recordings will be used to evaluate the thermal conductivity and BHE resistance with the same accuracy of conventional tests.

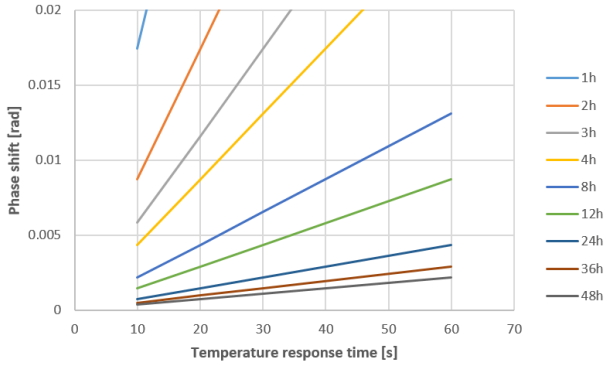

Fig. 2 Detectable phase shift as a function of the response time of the temperature sensors (periods from 1 to 48 h).

Acknowledgments

This research is funded by the Natural Science and Engineering Research Council of Canada (NSERC) through an Idea to Innovation grant awarded to J. Raymond and L. Lamarche.

References

COMSOL Multiphysics® (2019), v. 5.4., www.comsol.com. COMSOL AB, Stockholm, Sweden.

Guiltinan E. and Becker MW. (2015) "Measuring well hydraulic connectivity in fractured bedrock using periodic slug tests", Journal of Hydrology, 521, 100-107. doi: 10.1016/j.jhydrol.2014.11.066.

Kavanaugh SP. (2001), "Investigation of methods for determining soil formation thermal characteristics from short term field tests", ASHRAE RP-1118, Atlanta, USA.

Kurevija T., Macenić M. and Strpić K. (2018), "Steady-state heat rejection rates for a coaxial borehole heat exchanger during passive and active cooling determined with the novel step thermal response test method", Rudarsko-geološko-naftni zbornik, 33(2), 61-71. doi: 10.17794/rgn.2018.2.6

Oberdorfer P. (2014) "Heat transport phenomena in shallow geothermal boreholes – Development of a numerical model and a novel extension for the thermal response test method by applying oscillating excitations", Phd Thesis, Göttingen University.

Raymond J., Lamarche L. and Malo, M. (2015), "Field demonstration of a first thermal response test with a low power source", Applied Energy, 47, 30-39. doi: 10.1016/j.apenergy.2015.01.117

Spitler JD. and Gehlin S. (2015) "Thermal response testing for ground source heat pump systems - An historical review", Renewable and Sustainable Energy Reviews, 50, 1125-1137. doi: 10.1016/j.rser.2015.05.061

Stability analysis of a potential geothermal well in fractured porous media

Sina Heidari[1], Biao Li[1], Attila M. Zsaki[1], Baohong Yang[2], Bin Xu[1,3]

[1]Concordia University, Department of Building, Civil & Environmental Engineering, Montreal, Canada
[2]CGG, Geoscience Reservoir Americas, Calgary, Canada
[3]Origin Geomechanics Inc., Calgary, Canada
s_eidari@encs.concordia.ca

DOI: https://doi.org/10.5281/zenodo.3566016

Keywords: Dual-porosity medium, fractured strength, pore pressure, wellbore stability, analytical solution

Abstract

Deep geothermal engineering is usually involved in fractured reservoirs with high permeability and boreholes are usually inclined to promote thermal production. Wellbore stability is particularly important in such fractured porous media. In this paper, dual-porosity and dual-permeability theories of poromechanics are employed to study the stability of a potential geothermal well using analytical solutions. The effective stresses in the rock matrix and fractures surrounding the borehole are derived and analyzed separately, where two failure criterions are applied to rock matrix and fracture, respectively. Time-dependent solutions are used to show the importance of including fracture strength in stability analysis of wellbores drilled in fracture porous media.

1. Introduction

Understanding the behavior of naturally fractured media is an indispensable task in field operations of oil and gas industry. Inclined wellbore instability issues due to the local heterogeneity of surrounding rock is of critical interest. General methods of analysis in a 3D state which is based on elastic approach proposed by Hiramatsu and Oka (1968) and Bradley (1979) do not encompass the precise mechanisms of collapse initiation. Based on their application, wellbores are buried in a deep depth in which the formation is saturated. Fractures provide low porosity-high permeability environment which induces local preference for flow and fluid-diffusion. Coupled equations which can account fluid pressure perturbation and deformation of the rock are needed. Fractured rock was usually modeled as a dual-porosity/dual-permeability porous media (Abousleiman and Nguyen 2005). The analytical solutions by Abousleiman and Nguyen (2005) accurately capture the stresses and the pore-pressure variations in rock matrix and fracture for wellbore stability analysis. However, the effect of fracture strength on wellbore stability was not considered. In this paper we employ the poromechanics/poroelastic analytical solutions of Abousleiman et al (2005) to demonstrate the importance of considering fracture strength in the borehole stability analysis of a potential geothermal well.

2. Methods and techniques

Dual-porosity concept can be described by a representative elementary volume (REV). The chosen REV as shown in **Fig. 1** describes the rock matrix as well as the embedded fractures distribution. At the macroscopic level, the system is considered to consist of two separate and overlapping fluid-saturated porous media: one represents the primary porosity matrix and the other represents the secondary porosity medium fractures. Each medium is assumed to have its own poromechanical and physical properties such as elastic moduli, Biot's effective stress coefficients, and fluid mobilities. The two media communicate and may exchange fluid mass. At any REV, it is assumed that there are two separate continua, each with its own pressure field and separate constitutive laws and governing equations are considered for each region. The overall strain tensor is governed by the applied total stress tensor, and the dual pore pressure system. Pore pressures of each continuum are weighted by their own Biot's constants. For the proposed REV, the stresses and strains tensors are same for both matrix and fracture under the assumption that each porous medium is homogeneous and isotropic. Here subscripts I and II refers to matrix and fracture media respectively, and α^{I} and α^{II} are Biot's effective stress coefficients in matrix and fracture respectively.

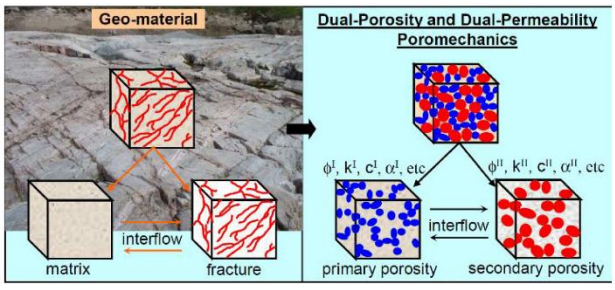

Fig. 1 Dual Porosity/dual permeability concept of poroelastic media. (Cowin et al 2009).

The complete analytical solution for the inclined wellbore drilled fractured-rock formation are given as follows:

$$P^{I} = p_0 + P^{I(2)} + P^{I(3)} \quad (1)$$

$$P^{II} = p_0 + P^{II(2)} + P^{II(3)}$$

$$\sigma_{rr} = \sigma_m - \sigma_d \cos\left[2(\theta - \theta_r)\right] - \sigma_{rr}^{(1)} - \sigma_{rr}^{(2)} - \sigma_{rr}^{(3)} \quad (2)$$

$$\sigma_{\theta\theta} = \sigma_m + \sigma_d \cos\left[2(\theta - \theta_r)\right] - \sigma_{\theta\theta}^{(1)} - \sigma_{\theta\theta}^{(2)} - \sigma_{\theta\theta}^{(3)} \quad (3)$$

σ_m and σ_d are mean and deviatoric stresses around the wellbore, p_0 denotes the virgin formation pore pressure before excavation which is assumed to be equal to both matrix and fracture virgin pore pressure at $r = \infty$. An example for dual porosity analytical solutions by Abousleiman and Nguyen (2005) is solved. Parameters are shown in **Table 1**. The solution in time is evaluated by a popular numerical inversion method which is Stehfest algorithm (Stehfest, 1970). For this case we use MATLAB to solve the Laplace equations. For the complete explanation of constitutive equations reader is referred to Abousleiman et al (2005).

Table 1 Rock-fluid properties for dual porosity modelling from Abousleiman and Nguyen (2005).

Parameter	Value
K^I, K^{II}	1100, 550 (MPa)
G^I, G^{II}	760, 380 (MPa)
K_s	27570 (MPa)
K_f	1744 (MPa)
ϕ^I, ϕ^{II}	0.14, 0.014
k^I, k^{II}	1e-19, 1e-17 (m^2)
p_0	10 (MPa)
R	0.1 (m)

Where R is radius of the well, K_s and K_f are grain bulk modulus and fluid modulus. ϕ^I and ϕ^{II} are matrix and fracture porosity, k^I and k^{II} are permeability of matrix and fracture respectively. We use different mud pressures to evaluate the response of media but as a first try it is assumed zero.

3. Results and discussions

Results of pore pressures are shown in **Fig. 2**. It shows that the pore pressure of fracture dissipates faster due to its high permeability. With the dual porosity solution, the pore pressure of matrix behaves differently when comparing with the single porosity solution.

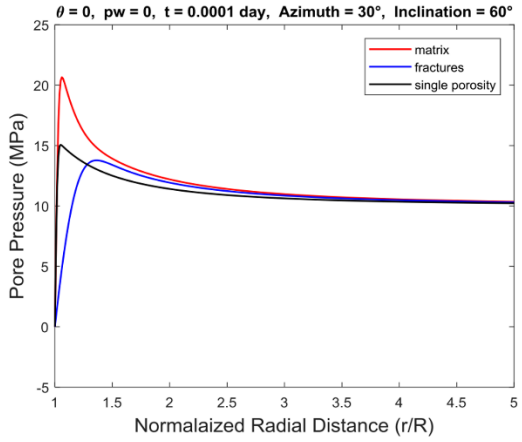

Fig. 2 Pore pressure values along radial direction.

Pairs of S_p versus $\sqrt{J_2}$ can be plotted to evaluate the stability of the well. These pairs are plotted along the whole periphery of the wellbore in which θ varies from 0 to 360 degree. Stress clouds show mean shear stress which can be compared by a failure criterion like Drucker-Prager.

$$J_2 = \frac{1}{6}\left[(\sigma_{rr} - \sigma_{\theta\theta})^2 + (\sigma_{rr} - \sigma_{zz})^2 + (\sigma_{\theta\theta} - \sigma_{zz})^2\right] + \sigma_{r\theta}^2 + \sigma_{rz}^2 + \sigma_{\theta z}^2 \quad (4)$$

$$S_p = \frac{\sigma_{rr} + \sigma_{\theta\theta} + \sigma_{zz}}{3} - p^I \quad (5)$$

Fig. 3 shows the analysis which evaluate the time factor. It can be seen that as time passes, the stress cloud expands and most parts of the wellbore get failure at t=1 day. We replaced the pore pressure of matrix with fracture pore pressure instead to figure out the role of low pore pressure generated in fractures Eq. 6.

$$S_p = \frac{\sigma_{rr} + \sigma_{\theta\theta} + \sigma_{zz}}{3} - p^{II} \quad (6)$$

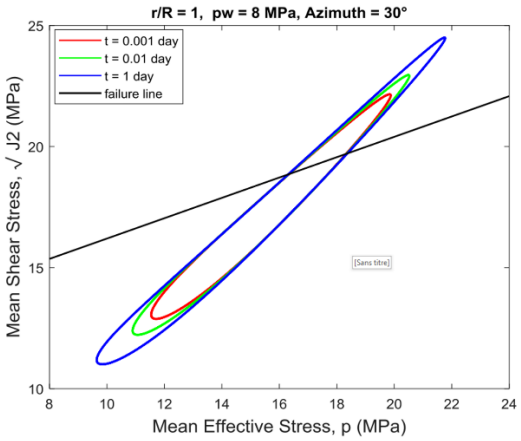

Fig. 3 Effect of different times on stress clouds at r/R=1 within a constant mud pressure.

In addition, due to the fact that rock formations contain weak plans like bedding planes (Nguyen et al 2009), presence of fractures and bedding planes needs modified failure criteria, in this manner the amounts of φ and c get reduced. Blue line in **Fig. 4** shows the modified failure line as to compare with fracture stress cloud. It is observed that fracture pore pressure makes a little difference but only one failure criteria based on the specific φ and c values for the whole formation is not enough.

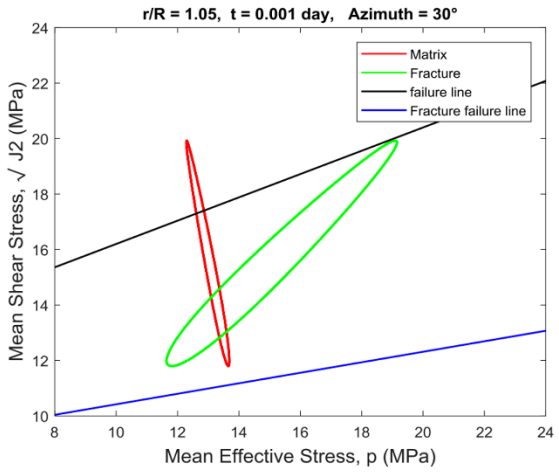

Fig. 4 Matrix and fracture stress clouds

4. Conclusions

In this paper we utilize dual-porosity concept available in the literature to emphasize the importance of such model in geothermal industry or any engineering career involved with borehole excavations. Parametric studies using MATLAB code shows that radial stress and pore pressure values are highly dependent on material properties like permeability and porosities of both matrix and fracture. After the early time following excavation, the amount of pore pressure is different in fracture and matrix and this fact clearly shows the importance of using dual-porelastic solution and the necessity of considering the fracture strength.

5. Acknowledgments

First author has benefited from international award of excellence provided by Concordia University, Montreal, QC. The Student Travel Assistance award to the first author by INRS is also acknowledged.

References

Abousleiman, Y. and Ekbote, S. 2005. Solutions for the Inclined Borehole in a Porothermoelastic Transversely Isotropic Medium. J. Appl. Mech. 72 (1): 102–114. doi:10.1115/1.1825433.

Abousleiman, Y. and Nguyen, V. 2005. PoroMechanics Response of Inclined Wellbore Geometry in Fractured Porous Media. J. Eng. Mech. 131(11): 1170–1183. doi:10.1061/(ASCE)0733-9399(2005)131:11(1170).

Bradley, W. B. 1979. "Failure of inclined boreholes." J. Energy Resour. Technol., 101, 232–239.

Cowin, S.C., Gailani, G., and Benalla, M. 2009. Hierarchical Poroelasticity: Movement of Interstitial Fluid Between Porosity Levels in Bones. Phil. Trans. R. Soc. A, 367: 1-44.

Hiramatsu, Y. and Oka, Y. 1968. Determination of the Stress in Rock Unaffected by Boreholes or Drifts, from Measured Strains or Deformations. Int. J. Rock Mech. Min. Sci., 5: 337–353.

Nguyen, V.X., Abousleiman, Y.N., and Hoang, S.K. 2009. Analyses of Wellbore Instability in Drilling Through Chemically Active Fractured Rock Formations. SPE J., 14(2): 283-301. SPE-105383-PA.

Stehfesh, H. 1970. Numerical Inversion of Laplace Transforms. Commun. ACM., 13: 47-49.

Alberta precambrian basement: implications for EGS development

Spencer Poulette[1]

[1]University of Alberta, Earth and Atmospheric Science, Edmonton, Canada

DOI: https://doi.org/10.5281/zenodo.3566024

Keywords: EGS, Alberta, crystalline rock, specific surface area

Abstract

The Precambrian basement underlying the Western Canadian Sedimentary Basin has recently become the subject of geothermal study. In order to implement an enhanced geothermal system in the Alberta Precambrian Basement, one must first understand the reactivity potential and the potential of the in-situ rocks to transmit fluid. In this paper, we present data pertaining to the specific surface areas of the basement rocks and the implications for EGS development. This opens the pathway for future research into the development of an EGS system in the basement rocks.

1. Introduction

The Alberta Precambrian basement underlies the Western Canadian Sedimentary Basin, ranging from a maximum depth of approximately six kilometers in the West, to outcropping at the surface in the Northeastern portion of the province. The basement rocks range in age from 1.7 billion, to 3.5 billion years old as determined through monazite and zircon ages (Ross 2002, Pană 2003). The lithologies that underlie the basement are dominantly crystalline, with protoliths being of both igneous and clastic sedimentary origin. Grades of metamorphism range from lower greenschist to upper amphibolite facies (Pană 2003) and almost all rocks display some characteristics of alteration by hot fluids.

The Alberta Precambrian basement has a limited dataset of cored wells which have intersected the basement due to extensive oil and gas exploration in the basin since the mid twentieth century. Thus, tectonic subdivisions of the basement have been determined on the basis of gravimetric and aeromagnetic survey data. From this, Ross (1990) divided the basement into 22 terranes and inferred several magmatic and shear zones. There are many terranes for which there is no core available, and future exploration into those terranes' geothermal potential may be warranted.

Previous works by Banks and Harris (2014) wherein basement rock properties were determined through analysis of their natural permeabilities and porosities have laid the groundwork for the determination of EGS potential. In their works, they also determined the lithologies of basement cores taken from within the Talston Magmatic Zone on the south shores of Lake Athabasca. It was determined that natural hydrological characteristics were not sufficient for fluid flow, and as such, an enhanced geothermal system would be necessary for geothermal development in many areas of Alberta. This is also due to the fact that the basin does not typically possess a geothermal gradient high enough to produce temperatures above 120°C within sedimentary rocks.

Due to the immense cost which an EGS would require, one must be assured of the level of reactivity of the basement rocks in order to avoid precipitation of unwanted minerals. This level of reactivity may be predicted qualitatively through the usage of specific surface area measurements. These measurements are of how much surface area of the rock is available to react with surrounding fluids and either dissolve or react with the fluid. Additionally, identifying the mineralogy of the rocks is of use as one may be able to predict reactions and dissolution occurring within the reservoir.

2. Methods and techniques

Six wells were identified as being of interest and were analyzed using various methods. Specific surface areas of basement rocks were determined by using the Autosorb IQ BET machine, which measures the specific surface area of the samples based on the adsorption and desorption characteristics of the sample. Rock samples were powdered to a consistent grain size, and two grams of powder were then analyzed. Additionally, thin section analysis and electron microprobe data were obtained in order to determine the composition of these basement rocks.

3. Results

The results of the specific surface area measurements for the six wells can be found in **Table 1**. Thin section analysis of these basement rocks details pervasive alteration due to fluid-rock interaction in many samples. Pyrite, hematite, and sericite are the dominant alteration products identified through thin section analysis. All wells show some degree of alteration, with at least one of the aforementioned phases present.

Table 1 Specific Surface Areas of Alberta Precambrian Basement Rocks.

Well Number	Lithology	Specific Surface Area (m^2/g)
1	K-mica Chlorite Biotite Gneiss	2.0981
2	Chloritized Paragneiss	3.8670
3	Biotite Chlorite Gneiss	0.5854
4	Biotite Gneiss	2.9622
5	Altered Metasediment	4.9199
7	Orthogneiss	0.5215

Electron microprobe data was obtained for four wells which were of interest. It was found that within several wells which possessed infilled fractures, the minerals infilling fractures were quartz, calcite, phengite, clinozoisite, pyrite, and clays.

4. Discussion

Previous works which have laid the groundwork for the development of an EGS have already showed that stimulation of the reservoir is a necessity for fluid flow. However, whether or not chemical stimulation would be effective was not clear. With a more accurate representation of vein mineralogy given by electron microprobe and thin section analysis here, an effective chemical stimulation plan may be able to be performed. However, without full core and fracture data analyses, it may be difficult to quantify the effect which that stimulation would have on the reservoir.

Specific surface areas of the basement rocks are within a wide range and reflect the heterogeneity and complexities of the geological history of the Alberta Precambrian Basement. It can be stated that those wells with a high specific surface area have more evidence of alteration than those without large amounts of alteration products. Additionally, mafic lithologies have a higher specific surface area than felsics, which is to be expected as mafic rocks are typically more reactive than felsic rocks. This increased specific surface area in specific wells would likely lead to more dissolution in the reservoir and thus increased precipitation in the system, decreasing effectiveness. It can be inferred that unaltered felsic rocks will make more effective reservoir than altered mafic rocks.

5. Conclusions

Basement rocks properties have been compiled on six wells which intersect the Alberta Precambrian Basement, resulting in a sound foundation for future study into the possibility of an EGS. There exists a natural fracture system within the basement in many wells, but the fractures have been infilled with mostly quartz, calcite, phengite, clinozoisite, pyrite, and clay minerals being the dominant phases. Additionally, specific surface areas of these rocks were determined, and the trend was for those rocks with more pervasive alteration to have a higher specific surface area. The potential for an effective geothermal system within the Alberta Precambrian Basement is much higher than the basin in many cases, and as such, warrants further investigation.

Acknowledgments

Funding for this project was provided by Future Energy Systems and COSIA. I would like to acknowledge the assistance and works of Dr. Jonathan Banks, Dr. Nick Harris, and Samuel Johnson for their contributions to this project.

References

Pană, D., Precambrian Basement of the Western Canada sedimentary basin in Northern Alberta, Alberta Energy and Utilities Board, Alberta Geologic Survey, 2003

Ross, G. M., Parrish, R. R., Villeneuve, M. E. and Bowring, S. A., Geophysics and geochronology of the crystalline basement of the Alberta Basin, western Canada Canadian Journal of Earth Sciences, Canadian Science Publishing, 1991, Vol. 28(4), pp. 512-522

Banks, J., Harris N., Developing Alberta's Geothermal Reserves with the EGS-CO2 Method, 2014

Ross, G. M. (2002). Evolution of Precambrian continental lithosphere in western Canada: Results from lithoprobe studies in Alberta and beyond. Canadian Journal of Earth Sciences, 39(3), 413-437.

Preliminary modelling of deep geothermal energy use in the Bécancour area (Québec)

Violaine Gascuel[1], Félix-Antoine Comeau[1], Christine Rivard[2], Jasmin Raymond[1]

[1]Institut national de la recherche scientifique, Centre Eau-Terre-Environnement, Québec, Canada
[2]Ressources naturelles Canada, CGC Québec, Québec, Canada
violaine.gascuel@ete.inrs.ca

DOI: https://doi.org/10.5281/zenodo.3566028

Keywords: St. Lawrence Lowlands, sedimentary basin, numerical modeling, heat production, low enthalpy

Abstract

Located in the St. Lawrence Lowlands sedimentary basin (Southern Québec), Bécancour is a populated area, hosting an industrial park. This project is to assess if using the deep saline aquifers (1 to 2 km deep) for heating purposes would be feasible. Uncertainty on the reservoir properties is the biggest hurdle for deep geothermal projects (e.g.: permeability, varies between $4x10^{-13}$ and 10^{-17} m^2 in the aquifers). Thus, efforts have been made to characterize the aquifers using vintage oil and gas wells in the area. New concepts of closed loops, standing column wells and doublets are being investigated to maximize efficiency.

1. Introduction

Geothermal heating from deep hydrothermal reservoirs is a reliable source of energy, enabling a reduction in greenhouse gases as well as economic growth (Jiang et al. 2019). Deep doublet systems have been used for half a century for district heating in the Paris Basin, France, showing sustainable performances over the long-term (Lopez et al. 2010). Deep closed loop systems (DBHE) have alternatively been developed in areas where formation permeability was insufficient for well doublets (Sapinska-Sliwa et al. 2016)

In Canada, geothermal energy is mostly used for heating and cooling purposes, including mostly shallow geothermal heat pump systems operated at low temperature (Raymond et al. 2015). Deep geothermal potential was studied with the aim of developing power plants (Majorowicz & Grasby 2010; Minea & Majorowicz 2012; Hofmann et al. 2014; Bédard et al. 2016; Richard et al. 2016). However, few studies have considered the heating potential for heating from hydrothermal resources at moderate depth (1 to 2 km).

The Bécancour area, selected for this study, is located in the St Lawrence Lowlands in southern Québec (Canada). This study area was chosen because there are potential large consumers for heat. Moreover, several oil and gas exploration wells were drilled in this area, whose data will be available for this project. The St. Lawrence Lowlands have additionally been studied for their geothermal (Gauchat 2017; Bédard et al. 2018) and CO_2 sequestration potentials (eg:Ngoc et al. 2014).

2. Methods

Preliminary models have already been built within the framework of this study. The performance of 1215 m deep open loop targeting the Cairnside unit and 1500 m deep U tubes DBHE designs were compared to heat an industrial building (set heat requirements). They were developed to test the types of deep geothermal heat exchangers that could be implemented in this area, their requirements and expected performances.

For these preliminary models, all geological units of the St. Lawrence Lowlands were considered homogeneous and horizontal. The depth, unit permeability and brine properties were based on work by eg:Tran Ngoc et al. (2014). Thermal conductivity, heat capacity and density of the different units were defined according to (Bédard et al. 2018) .

Models were run in 3D using the FEFLOW finite element software, assuming a constant surface temperature of 8 °C, and constant bottom temperature calculated using the temperature gradient found in Tran Ngoc et al. (2014). A constant hydraulic head was imposed on lateral boundaries, which were considered adiabatic for heat transfer. Fluid flow was solved in steady state (with transient temperature transport) as data on storage capacity was unavailable. Doublets were modelled as a 1D vertical boundary of constant temperature (8°C) and constant flow (corresponding to the yearly mean of pumping flow needed to respond to heat demand). DBHE were modeled as 1D vertical boundary with imposed heat flux (varying monthly to reproduce the heat requirements). The heat requirement was equally divided between nodes of the DBHE. Mass transport and thermal conductivity dependence on temperature and pressure were not considered.

3. Results

Two types of systems appear technically feasible when considering mean hydraulic and thermal properties: 1) an open loop system with a spacing of 200 m between pumping and injection and 2) a DBHE, with 3 wells to provide the required 780 kW. However, the sensitivity study showed that if permeability falls on the lower side

of expected values, pumping and reinjecting in the open loop would require too much power to be technically possible (Fig. *1*).

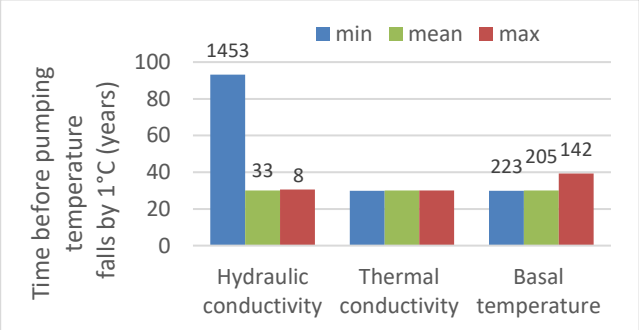

Fig. 1 Sensitivity of thermal breakthrough for an open loop system in the Cairnside unit with 200 m between pumping and injection. Numbers over hydraulic conductivity correspond to maximum drawdown (m) after 30 years of operation. Numbers over basal temperature correspond to the mean pumping rate (m^3/d).

4. Discussion

The preliminary models, developed at an early stage of a PhD thesis, used simplified geometry, properties and physics. Further work will use more complex models and specific properties to the Bécancour area, including historical data on brine extraction. Overlying units with reservoir potential (Beekmantown, Trenton), as well as different DBHE configurations, will also be considered.

5. Conclusions

The simulated open loop system within the Cairnside Formation appears to be the simplest design to meet the heat requirement. However, its feasibility is highly dependent on the permeability of the unit, which is known to be heterogenous (Tran Ngoc et al. 2014). Further work will offer insights into the performance of the different geothermal system, based on investigation of the formation properties and numerical modelling of various designs.

Acknowledgments

This project is funded by the Geological Survey of Canada (GNES program).

References

Bédard, K., Comeau, F.-A., Millet, E., Raymond, J., Malo, M., & Gloaguen, E. (2016). *Évaluation des ressources géothermiques du bassin des Basses-Terres du Saint-Laurent*. Québec: Institut national de la recherche scientifique. found at http://espace.inrs.ca/4845/

Bédard, K., Comeau, F.-A., Raymond, J., Malo, M., & Nasr, M. (2018). Geothermal Characterization of the St. Lawrence Lowlands Sedimentary Basin, Québec, Canada. *Natural Resources Research, 27*(4), 479-502. doi: 10.1007/s11053-017-9363-2. found at https://doi.org/10.1007/s11053-017-9363-2

Gauchat, L. (2017). *Analyse de la fracturation et de la perméabilité des grès du Groupe de Potsdam face aux ressources géothermiques profondes* (Université du Québec, Institut national de la recherche scientifique).

Hofmann, H., Weides, S., Babadagli, T., Zimmermann, G., Moeck, I., Majorowicz, J., & Unsworth, M. (2014). Potential for enhanced geothermal systems in Alberta, Canada. *Energy, 69*, 578-591. found at https://doi.org/10.1016/j.energy.2014.03.053.

Jiang, Y., Lei, Y., & Liu, J. (2019). Economic Impacts of the Geothermal Industry in Beijing, China: An Input–Output Approach. *Mathematical Geosciences, 51*(3), 353-372. doi: 10.1007/s11004-019-09787-8. found at https://doi.org/10.1007/s11004-019-09787-8

Lopez, S., Hamm, V., Le Brun, M., Schaper, L., Boissier, F., Cotiche, C., & Giuglaris, E. (2010). 40 years of Dogger aquifer management in Ile-de-France, Paris Basin, France. *Geothermics, 39*(4), 339-356. found at https://doi.org/10.1016/j.geothermics.2010.09.005.

Majorowicz, J., & Grasby, S. E. (2010). High potential regions for enhanced geothermal systems in Canada. *Natural Resources Research, 19*(3), 177-188. found at https://doi.org/10.1007/s11053-010-9119-8.

Minea, V., & Majorowicz, J. (2012). Preliminary assessment of deep geothermal resources in Trois-Rivieres area, Quebec. *Geothermal Resources Council Transactions, 36*, 709-715.

Ngoc, T. T., Lefebvre, R., Konstantinovskaya, E., & Malo, M. (2014). Characterization of deep saline aquifers in the Bécancour area, St. Lawrence Lowlands, Québec, Canada: implications for CO 2 geological storage. *Environmental Earth Sciences, 72*(1), 119-146.

Raymond, J., Malo, M., Tanguay, D., Grasby, S., & Bakhteyar, F. (2015). Direct utilization of geothermal energy from coast to coast: a review of current applications and research in Canada. Dans *Proceedings of the World Geothermal Congress*.

Richard, M.-A., Giroux, B., Gosselin, L., Kendall, J., Malo, M., Mathieu-Potvin, F., . . . Raymond, J. (2016). Intégration de la géothermie profonde dans le portefeuille énergétique canadien: Hydro Québec, Institut de recherche.

Sapinska-Sliwa, A., Rosen, M. A., Gonet, A., & Sliwa, T. (2016). Deep borehole heat exchangers—A conceptual and comparative review. *International Journal of Air-Conditioning and Refrigeration, 24*(01), 1630001.

Tran Ngoc, T. D., Lefebvre, R., Konstantinovskaya, E., & Malo, M. (2014). Characterization of deep saline aquifers in the Bécancour area, St. Lawrence Lowlands, Québec, Canada: implications for CO2 geological storage. *Environmental Earth Sciences, 72*(1), 119-146. found at http://dx.doi.org/10.1007/s12665-013-2941-7.

GEOTHERMAL CANADA

UNIVERSITY OF WATERLOO

UNIVERSITY OF ALBERTA

UNIVERSITÉ LAVAL

DEEP CORP.

DEEP | EARTH | ENERGY | PRODUCTION

AQPER

ASSOCIATION QUÉBÉCOISE
DE LA PRODUCTION
D'ÉNERGIE RENOUVELABLE